1 Two Ubiquitin-Activating Systems Occur in Plants with One Playing a Major Role 2 in Plant Immunity 3 Bangjun Zhou<sup>a</sup>, Chaofeng Wang<sup>a,†</sup>, Xuanyang Chen<sup>b,2,†</sup>, Yi Zhang<sup>a,1</sup>, and Lirong Zeng<sup>a,\*</sup> 4 5 <sup>a</sup>Plant Science Innovation Center and Plant Pathology Department, University of 6 Nebraska, Lincoln, NE 68588 <sup>b</sup>Biology Department, University of Arkansas, Little Rock, AR 72204 7 <sup>1</sup>Present address: South China Botanical Garden, Chinese Academy of Sciences, 8 9 Guangzhou 510650, China <sup>2</sup>Present address: Department of Agronomy, Fujian Agriculture and Forestry University, 10 11 Fuzhou, 35002, China <sup>†</sup>These authors contribute equally to this work 12 \*Address correspondence and material requests to lzeng3@unl.edu 13 Running title: Plants possess dual ubiquitin-activating systems 14 15 16 One sentence summary: Plant dual ubiquitin E1 systems play distinct roles in plant 17 immunity by differentially charging the ERAD-associated E2s for ER stress tolerance. 18 19 **Corresponding Author:** Lirong Zeng University of Nebraska-Lincoln 20 1901 Vine St 21 22 Lincoln, NE 68588 23 (402) 472-2539 (voice) Email: lzeng3@unl.edu 24 25 Authors' email address: Bangjun Zhou bzhou3@unl.edu 26 27 Chaofeng Wang cwang53@unl.edu Xuanyang Chen cxy1991@163.com 28

Yi Zhang yizhang@scbg.ac.cn

29

30

#### **Abstract**

31

32

33

34

35

36

37

38

39

40

41

42

43

44

45

46

47

48

Many plants possess two or more ubiquitin-activating enzymes (E1). However, it is unclear whether the E1s of a plant genome play equivalent roles in various pathways. Here we report that tomato and tobacco encode dual ubiquitin-activating systems (DUAS) in which the E1s UBA1 and UBA2 display differential specificities in charging four groups of E2s. The C-terminal ubiquitin-folding domain of the E1s play a major but not sole role in determining the differential specificities of charging the four groups E2s. The dual systems do not play equivalent roles in plant immunity, with silence of UBA2 only compromising host immunity. Among the differentially charged E2s, group IV members UBC32, UBC33 and UBC34 are shown to be essential for ER-associated protein degradation (ERAD) and plant immunity. Like tomato, Arabidopsis UBC32/33/34 E2 triplet are also differentially charged by its E1s and are essential for plant immunity. Loss of function in Arabidopsis UBC32, UBC33 and UBC34 does not affect flg22 and elf18triggered inhibition of seedling growth but results in alteration of ER stress tolerance, which likely contribute to the diminished plant immunity in the mutants. Our results uncover DUAS in plants and a previously unknown E1-ERAD-associated E2 triplet module in the regulation of host immunity.

#### Introduction

Ubiquitination is a post-translational protein modification (PTM) that plays key roles in numerous cellular and physiological processes. The stepwise enzymatic cascade catalyzing ubiquitination typically consists of three different classes of enzymes, ubiquitin-activating (E1), ubiquitin-conjugating (E2), and ubiquitin ligase (E3) (Callis, 2014). In the E1-E2-E3 cascade, E1s stand at the apex thus modification of proteins by ubiquitin depends on the abundance, activity, and specificity of the E1 enzymes (Schulman and Harper, 2009).

Humans possess dual E1 activation systems for ubiquitin that are directed by two distantly-related E1 enzymes UBE1 and UBA6 (Jin et al., 2007). The UBA6 and UBE1 display distinct preferences for E2 charging in vitro, with the E1-E2 specificity depending partly on their C-terminal Ufd domain, which is similar to that of the yeast E1 (Jin et al., 2007; Lee and Schindelin, 2008; Olsen and Lima, 2013). The UBA6 orthologues were detected in vertebrates and the echinoderm sea urchin but not in insects, worms, fungi, and plants (Jin et al., 2007). In plants, homologs of human UBE1 have been isolated with ubiquitin-activating activity being demonstrated from wheat (Hatfield and Vierstra, 1992), Nicotiana tabacum (Takizawa et al., 2005), Arabidopsis (Hatfield et al., 1997) and soybean (Zhang et al., 2018). While most plant species encode two or more Els, it remains unknown whether the plant Els have different specificities for E2 charging. Neither has been elucidated whether and how different ubiquitin E1s from a given plant genome play different roles. In N. tabacum, expression of the two E1 genes, NtUBA1 and NtUBA2 was induced in response to viral infection, wounding, and defenserelated hormones, leading to the speculation that they might play equal roles in stress responses (Takizawa et al., 2005). However, the two Arabidopsis E1 enzymes apparently function differentially in plant responses to biotic stress (Goritschnig et al., 2007).

In eukaryotes, endoplasmic reticulum-associated protein degradation (ERAD) is part of the ER-mediated protein quality control (ERQC) machinery, which includes chaperone-mediated assistance in protein folding and the selective degradation of terminally misfolded proteins by ERAD (Buchberger et al., 2010; Li et al., 2020). The terminally

misfolded proteins are first recruited by adapters such as the HRD3 protein, to different ER membrane-anchored E3 ligase complexes, such as the HRD1 (HMGCOA Reductase Degradation 1) and the DOA10 (Degradation Of Alpha2 10) complex, followed by retrotranslocation, ubiquitination, and subsequent 26S proteasome-dependent degradation in the cytoplasm (Buchberger et al., 2010; Strasser, 2018). Failure to remove misfolded proteins by ERAD is associated with more than sixty human diseases, including neurodegenerative diseases, diabetes, and cancer (Guerriero and Brodsky, 2012). ERAD has also emerged in recent years to play an important role in modulating plant responses to biotic and abiotic stress (Chen et al., 2020). In Arabidopsis, the E2 enzyme AtUBC32 serves as an active ERAD component and functions in the salt stress tolerance (Cui et al., 2012b). Although the E2 enzymes AtUBC33 and AtUBC34 were also shown to be localized to the ER membrane (Ahn et al., 2018), evidence for the involvement of AtUBC33 and AtUBC34 in ERAD is lacking. To date, no ERAD-associated E2 enzymes have been reported to be involved in plant immunity.

In this study, we found that both tomato (Solanum lycopersicum) and Nicotiana benthamiana possess dual E1 ubiquitin-activating systems (DUAS) that are directed by two E1s, UBA1 and UBA2. The dual systems involve differential charging of four groups E2s and do not play equivalent roles in plant immunity and development. The C-terminal ubiquitin-folding domain to the tomato E1s were shown to play a major but not sole role in governing differential charging of the four groups E2s. Among the E2s that are differentially charged by the E1s are the group IV that consists of homologs to the Arabidopsis E2s AtUBC32, AtUBC33 and AtUBC34. The tomato and N. benthamiana UBC32, UBC33 and UBC34 are shown to be essential for ERAD and plant innate immunity. Noteworthy, AtUBC32, AtUBC33 and AtUBC34 are also found to be differentially charged by the Arabidopsis E1s and essential for host immunity, suggesting DUAS may be conserved in many plants. Loss of function in AtUBC32, AtUBC33 and AtUBC34 does not affect flg22 and elf18-triggered suppression of seedling growth but results in alteration of ER stress response, which likely contribute to the diminished plant immunity in the mutants. Additionally, the AtUBC32 and AtUBC33/34 appear to play

differential roles in ER stress response, suggesting complexity in the modulation of plant

immunity by the E1–group IV E2 triplet module.

112

113

#### Results

114

115

116

117

118

119

120

121

122

123

124

125

126

127

128

129

130

131

132

133

134

135

136

137

138

139

140

141

142

143

144

## **Tomato and Tobacco Genomes Each Encode Two Ubiquitin E1s**

The E1 enzymes possess a signature architecture that contains three conserved domains, a pseudo-dimeric adenylation domain involved in the ubiquitin activation, a Cys domain harboring the catalytic cysteine residue, and a ubiquitin-fold domain (Ufd) that participates in recruitment of E2 (Lee and Schindelin, 2008; Olsen and Lima, 2013; Schäfer et al., 2014). When the sequences of Arabidopsis and wheat ubiquitin E1 enzymes were used to search the tomato genome, two genes (Solyc06g007320) and Solyc09g018450) were identified that encode proteins containing all the conserved domains of E1 and with a deduced molecular mass of ~ 110 kilodalton (Supplemental Figure S1) (Hatfield and Vierstra, 1992; Hatfield et al., 1997; The tomato genome Consortium, 2012). The two genes were named SIUBA1 (Solanum lycopersicum <u>ubiquitin-activating</u> enzyme1) (Solyc06g007320) and SIUBA2 (Solyc09g018450), respectively in the order of being cloned. In vitro thioester assay (Kraft et al., 2005; Takizawa et al., 2005) showed that both SlUBA1 and SlUBA2 can catalyze formation of tomato E2 SlUBC3-ubiquitin adducts that is sensitive to DTT (Figure 1A), indicating they both possess ubiquitin-activating activity. N. benthamiana is a solanaceous species related to tomato and has served as an important model system for studying plant immunity. When sequences of SIUBA1 and SIUBA2 were used to search homologs in the N. benthamiana genome (Bombarely et al., 2012), two genes (Niben101Scf09017g00015 and Niben101Scf03202g13010) were found to encode proteins that contain all the hallmark E1 domains and to be highly homologous to SIUBA1 and SIUBA2, respectively. Consistent with earlier report (Jin et al., 2007), no homologous genes of human UBA6 were identified in the tomato and N. benthamiana genomes. Phylogenetic analysis indicated that SIUBA1 and SIUBA2 have the highest homology with NbUBA1 and NbUBA2, respectively (Supplemental Figure S2).

Most plant species possess two or more ubiquitin E1s (Supplemental Table I). To address whether the E1s of a given plant genome function equivalently or distinctly, we first analyzed the expression and subcellular localization of the two tomato E1 genes. Both *SlUBA1* and *SlUBA2* were expressed in all the tomato organs tested and no significant

difference in the level of expression was detected between SlUBA1 and SlUBA2 (Figure

1B). In addition, SlUBA1 and SlUBA2 both expressed in the nucleus and cytoplasm

147 (Figure 1C).

145

146

148

149

150

151

152

153

154

155

156

157

158

159

160

161

162

163

164

165

166

167

168

169

170

171

172

173

174

175

## SIUBA1 and SIUBA2 Play Different Roles in Plant Development and Immunity

To find out whether the two tomato E1s also function similarly, we silence the expression of the UBA1 and UBA2 gene in tomato and N. benthamiana by virus-induced gene silencing (VIGS) (Supplemental Figure S4). Based on the alignments of tomato and N. benthamiana UBA1 and UBA2 gene, we chose a fragment from SlUBA1 gene for specifically silencing tomato SlUBA1 and N. benthamiana NbUBA1, and a fragment from SlUBA2 gene for specifically silencing of SlUBA2 and NbUBA2 (Supplemental Figure S3). These two fragments were joined together for silencing both UBA1 and UBA2 in tomato and N. benthamiana. The UBA1 and UBA2 genes of tomato and N. benthamiana were silenced specifically and efficiently in TRV-UBA1, TRV-UBA2 and TRV-UBA1/2 infected plants (Supplemental Figure S4). Silencing of UBA1 and UBA2 caused growth changes in tomato and N. benthamiana plants. Both UBA1 and UBA2-silenced plants displayed reduced growth compared to the control plants (Figure 1D, 1E and Supplemental Figure S5). UBA1-silenced plants were dwarf with shorter nodes, a shorter taproot and fewer branch roots and slightly smaller leaves, whereas TRV-UBA2 infected plants were nearly as tall as the control plants and a shorter taproot and significantly fewer branch roots, and smaller, narrowly shaped leaves. Tomato and N. benthamiana plants where both UBA1 and UBA2 were silenced were severely affected in growth and development, rapidly etiolated and eventually died within five to seven weeks after TRV-UBA1/2 inoculation.

Expression of the tomato *UBA1* and *UBA2* genes is induced upon treatment of leaves with the immunogenic peptide of flagellin, flg22 (Supplemental Figure S6), suggesting they both are involved in host immunity. To find out whether the tomato and *N. benthamiana* E1s also play different roles in immunity, we employed two assays to evaluate plant pathogen-associated molecular pattern (PAMP)-triggered immunity (PTI) on *UBA1* and *UBA2*-silenced *N. benthamiana* plants. Cell death suppression assay

(CDSA) was first performed on UBA1 and UBA2-silenced and control N. benthamiana plants (Chakravarthy et al., 2010). In CDSA, PTI induced by the nonpathogen P. fluorescens 55 on the N. benthamiana plants inhibits the hypersensitive cell death induced by subsequent inoculation of *Pseudomonas syringae* pathovar *tomato* (*Pst*) strain DC3000 in the overlapping area (Figure 1F). However, our results showed that cell death was observed in the overlapping area on *UBA2*-silenced plants but not *UBA1*-silenced N. benthamiana plants, which implies a breakdown of PTI induction on UBA2-silenced plants. We further examined the effects of silencing UBA1 and UBA2 on restriction of Pst strains DC3000∆hrcQ-U and DC3000∆hopQ1-1 growth on tomato and N. benthamiana plants, respectively (Wei et al., 2007; Zhou et al., 2017). The T3SS (type three secretion system)-deficient Pst strain DC3000\(Delta hrcQ-U\) elicits PTI on tomato plants (Kvitko et al., 2009). Growth of DC3000∆hrcQ-U on the UBA2-silenced tomato plants was significantly higher at day 3 and day 4 after inoculation than that on the UBA1-silenced and TRV-infected control plants (Figure 1G). Pre-inoculation with the nonpathogen P. fluorescens 55 would induce PTI and enhance differences in pathogenic bacterial growth between wild-type and PTI-defective N. benthamiana plants (Nguyen et al., 2010). Accordingly, the growth of Pst DC3000 $\Delta$ hopQ1-1 on the UBA2-silenced plants was significantly higher than that on the UBA1-silenced and non-silenced control plants at day 3 and day 4 after inoculation (Figure 1H). Thus, our results confirmed that tomato and N. benthamiana UBA1 and UBA2 function differentially in host immunity.

# Tomato Possesses DUAS in which UBA1 and UBA2 Differentially Charge Four

### Groups of E2s

176

177

178

179

180

181

182

183

184

185

186

187

188

189

190

191

192

193

194

195

196

197

198

199

200

201

202

203

204

205

206

E1s initiate the enzymatic cascade for ubiquitination by coordinating ubiquitin activation with transferring to cognate E2s. To find out the underlying molecular basis for differential roles of tomato E1s in host immunity, we examined the specificities of tomato UBA1 and UBA2 in charging of a panel of 34 tomato E2s (Zhou et al., 2017). The majority of the E2s tested can be charged by both SIUBA1 and SIUBA2 at comparable specificities (Figure 2A and Supplemental Figure S7, Supplemental Table II). By contrast, E2s in groups IV, V, VI, and XII were charged by SIUBA2 at significantly higher efficiency. In particular, the group V E2s were efficiently charged by SIUBA2 but not

207 charged (SIUBC7 and SIUBC36) or at extremely lower efficiency (SIUBC14 and

SIUBC35) by SIUBA1. Thus, tomato possesses dual E1 activation systems for ubiquitin.

209 Interestingly, the tomato group IV, V, and VI E2s that are differentially charged by

SIUBA1 and SIUBA2 are phylogenetically close to those human E2s that are also

differentially charged by human E1s UBE1 and UBA6 (Supplemental Figure S8).

- To find out if the Ufd domain also plays a role in differential E2 charging by plant E1s,
- we exchanged the Ufd domain of SlUBA1 and SlUBA2 to build chimeric SlUBA1 and
- 215 SlUBA2 proteins (SlUBA1-Ufd<sup>SlUBA2</sup> and SlUBA2-Ufd<sup>SlUBA1</sup>) (Supplemental Figure
- 216 S9A and S9B). The chimeric SlUBA1-Ufd<sup>SlUBA2</sup> and SlUBA2-Ufd<sup>SlUBA1</sup> proteins charged
- 217 the SIUBC3 (as control) at similar efficiency, which is the same as that when SIUBA1
- and SlUBA2 were used (Figure 1A). By contrast, E2s from group IV and V were charged
- by the chimeric SIUBA1-Ufd<sup>SIUBA2</sup> at much higher efficiencies, which is opposite to the
- results that SIUBA1 and SIUBA2 were used. Thus, the Ufd domain of tomato E1s also
- plays a major role in the specificity of E2 charging. The charging of E2s by SlUBA1-
- 222 Ufd<sup>SIUBA2</sup> is slightly weaker than by SIUBA2 (Figure 2A), suggesting the Ufd domain
- may not be the sole factor that determine the E2 charging specificities. This was further
- supported by the result that no difference was detected in the strength of interaction
- between the Ufd domain of SIUBA1 (Ufd<sup>SIUBA1</sup>) and SIUBA2 (Ufd<sup>SIUBA2</sup>) and the group
- 226 IV E2s (Supplemental Figure S9C).

210

211

212

227

228

### The SIUBA2 Has Higher Specificities Than SIUBA1 and Play A Major Role in

### 229 Charging Group IV E2s in vivo

- The distinct roles of tomato and *N. benthamiana* E1s in host immunity are likely due to
- 231 their differential specificities in charging of certain members of the four groups of E2,
- 232 which act with cognate E3s to target plant immune components. Considering the
- 233 involvement in numerous human diseases and the emerging role in plant immunity for
- ERAD and the involvement of AtUBC32 in ERAD (Cui et al., 2012b; Guerriero and
- Brodsky, 2012), we decided to focus on the group IV E2s for further characterization of
- 236 the plant DUAS. Higher specificity of an E1 in charging E2s would be manifested by
- stronger E1-E2 interaction, as the factors that govern affinity and specificity for a target

protein are the same (Eaton et al., 1995). We thus employed three different assays of E1-E2 interaction to test the specificities of SIUBA1 and SIUBA2 for group IV E2s in vivo. First, the yeast two-hybrid assay showed group IV E2s have much stronger interaction with SIUBA2 (Figure 2C). And the differential interactions were not caused by differential levels of protein expression (Figure 2C, right panel). Similarly, SlUBA2 has stronger interactions with group V E2s than that of the SIUBA1 in yeast two-hybrid (Supplemental Figure S10A). Next, much stronger in planta interaction of SIUBC32, SIUBC33, and SIUBC34 with SIUBA2 than with SIUBA1 was detected in the bimolecular fluorescence complementation (BiFC) assay (Figure 2D). The SIUBA1 and SIUBA2 protein as well as the corresponding E2 protein in each pair of SIUBA1-E2 and SIUBA2-E2 being compared were expressed at comparable level (Figure 2D, lower panel). Lastly, co-immunoprecipitation was employed to detect the interactions of the two tomato E1s with group IV E2s. As shown in Figure 2E and 2F, group IV E2s pulled down significantly more SlUBA2 than SlUBA1 in the assay. Together, these results indicate that SIUBA2 possesses higher specificity towards group IV E2s than that of SlUBA1 and likely plays a major role in charging the E2 triplet in vivo. To further corroborate this conclusion, we tested charging of the group IV E2s in planta by transient expressing myc-tagged E2s on N. benthamiana plants where either UBA1 or the UBA2 genes was silenced. Compared to the control plants, no noticeable difference in charging of group IV E2 was observed on the UBA1-silenced plants. By contrast, silencing of UBA2 essentially abolished the charging of the group IV E2s (Supplemental Figure S10B).

## **Group IV E2s Are Required for Plant Immunity**

238

239

240

241

242

243

244

245

246

247

248

249250

251

252

253

254

255

256

257

258

259

260

261

262

263

264

265

266

267

268

Quantitative PCR (qPCR) indicated that group IV E2 genes, *SlUBC32*, *SlUBC33* and *SlUBC34* were significantly induced two hours after flg22 treatment (Figure 3A) and 24 hours after inoculation of the tomato plants with *Pst* strains DC3000 (Figure 3B). The *SlUBC33* and *SlUBC34* were also induced at 24 hours after inoculation of DC3000\(Delta hrcQ-U\). Growth of the *Pst* strain DC3000\(Delta hrcQ-U\) was significantly higher on tomato plants in which the *SlUBC32*, *SlUBC33* and *SlUBC34* genes were efficiently knocked down by VIGS (Figure 3C) than that on the control (TRV) plants on day 3 after

inoculation (Figure 3D and Supplemental Figure S11A), suggesting that group IV E2s are required for plant immunity.

The *N. benthamiana* genome encodes a corresponding close homolog for each of the tomato E2s (Zhou et al., 2017). In order to confirm the roles of group IV E2s in plant immunity, we developed transgenic *N. benthamiana* lines in which group IV E2 genes are silenced. Among the group IV E2 genes, *UBC33* and *UBC34* are highly homologous but have relatively lower homology to *UBC32* (Zhou et al., 2017). Therefore, the transgenic lines UBC32i and UBC33/34i where the *UBC32* and the *UBC33/UBC34* gene are specifically silenced, respectively were developed (Figure 3E). Growth of the *Pst* strain DC3000Δ*hopQ1-1* on the *UBC32*-silenced (UBC32i) and *UBC33/34*-silenced (UBC33/34i) plants was significantly higher than that on the wild type *N. benthamiana* plants on day 3 after inoculation (Figure 3F). Consistently, silencing of *UBC32*, *UBC33* and *UBC34* in *N. benthamiana* plants by VIGS also resulted in reduced host immunity (Supplemental Figure S11B).

## Group IV E2s Are Localized to ER and Interact with ERAD-Related E3s

Similar to their Arabidopsis counterpart, tomato SIUBC32, SIUBC33 and SIUBC34 possess a conserved transmembrane domain (TMD) (Supplemental Figure S12) (Ahn et al., 2018). In Arabidopsis, ER-localized AtUBC32 interacts with the HRD1/HRD3A E3 complex to serve as part of the ERAD system (Cui et al., 2012b; Chen et al., 2016). SIUBC32, SIUBC33 and SIUBC34 fused with GFP to the C-terminus co-localized with the mCherry-fused, ER-localized Marker ER-rb (Nelson et al., 2007) in *N. benthamiana* leaves (Figure 4A), indicating they are also ER-bound. By contrast, the localization to ER was abolished when the TMD of SIUBC32, SIUBC33 and SIUBC34 was deleted. Next, we examined the interaction of group IV E2s with the tomato closest homolog of the ERAD-related E3s AtHRD1A and AtHRD1B. The tomato HRD1A (SIHRD1A) and HRD1B (SIHRD1B) are localized to the ER (Supplemental Figure S13). As shown in Figure 4B, SIUBC32, SIUBC33 and SIUBC34 all interact strongly with SIHRD1A, SIHRD1B and their adapter protein SIHRD3A in yeast two-hybrid assay using the mating-based split-ubiquitin system (mbSUS) (Grefen et al., 2009). To further confirm

the association of SIUBC32, SIUBC33 and SIUBC34 with E3 SIHRD1A and SIHRD1B,

the BiFC assay was performed using tomato protoplasts. SlUBC32, SlUBC33 and

SIUBC34 interacted with the SIHRD1A and SIHRD1B in the assay to generate green

fluorescence signals whereas no signals were detected in control (Figure 4C). These

results suggest that SIUBC32, SIUBC33 and SIUBC34 are also likely involved in ERAD.

### **UBA2** and Group IV E2s Are Required for ERAD

To confirm the involvement of group IV E2s in ERAD, we probed stability of the known

ERAD substrate protein MLO-12 under conditions that group IV E2 genes were

overexpressed or silenced (Muller et al., 2005; Cui et al., 2012b). Compared to the

control, transient co-expression of MLO-12 and individual member of the group IV E2s

promoted the degradation of MLO-12 (Figure 4D). By contrast, silencing of UBA2,

UBC32 and UBC33/34 by VIGS enhanced the accumulation of MLO-12 (Figure 4E),

suggesting that UBA2 and group IV E2s are required for ERAD. No increase of MLO-12

was observed in UBA1 gene-silenced N. benthamiana plants, which is consistent with the

results that UBA2 play a major role in charging the group IV E2s in vivo. Similarly, the

degradation of MLO-12 was diminished in the tobacco RNAi transgenic lines UBC32i

and UBC33/34i (Figure 4F). Taken together, these results confirm that group IV E2s are

active components of the ERAD system and both the group IV E2s and the UBA2 are

required for ERAD.

301

302

303

304

305

306

308

309

310

311

312

313

314

315

316

317

318

319

320

321

324

325

326

327

328

329

## AtUBC32, AtUBC33 and AtUBC34 Are Differentially Charged by Arabidopsis E1s

### and AtUBC33 and AtUBC34 Are Also Required for ERAD

323 To study the role of individual members of the group IV E2s in ERAD and host

immunity, we attempted to knock down each member specifically. However, the

extremely high homology between SIUBC33 and SIUBC34 makes it highly challenging

to silence them individually by VIGS or RNAi-based gene-silencing. Tomato group IV

E2s interact with Arabidopsis ERAD E3 AtHRD1A in vivo (Supplemental Figure S14).

In addition, Arabidopsis E1s AtUBA1 and AtUBA2 differentially charge tomato

SIUBC32 (Figure 5A). These results suggest that the function for tomato and Arabidopsis

330 UBC32, UBC33 and UBC34 in ERAD is likely conserved. Furthermore, AtUBA1

332

333

334

335

336

337

338

339340

341

342

343

344

345

346

347

348

349

350

351

352

353

354

355

356

357

358

359

360

charged AtUBC32, AtUBC33, AtUBC34, and SIUBC32 at much higher efficiencies than that of AtUBA2 (Figure 5B), indicating that Arabidopsis also possesses dual E1 activation systems for ubiquitin, with the Arabidopsis AtUBA1 being the ortholog of tomato SlUBA2. Finally, the Arabidopsis E1s AtUBA1 and AtUBA2 were also shown to be not equally required for disease resistance and a 15-bp deletion at the C-terminus of AtUBA1 in the mos5 mutant compromised host immunity (Goritschnig et al., 2007). The 15-bp/5- amino acid deletion in mos 5 AtUBA1 are mapped to the Ufd domain that is highly conserved among tomato, tobacco, and Arabidopsis E1s (Supplemental Figure S15). Thus, we decided to take advantage of the null mutant lines available for Arabidopsis AtUBC32, AtUBC33 and AtUBC34 gene for our study. We obtained mutant lines in which AtUBC32, AtUBC33, and AtUBC34 are knocked out (Supplemental Figure S16A) and generated homozygous double and triple mutant lines ubc32/33, ubc32/34, ubc33/34, and ubc32/33/34 by crossing and genotyping (Supplemental Figure S16B). The expression of the AtUBC32, AtUBC33 and AtUBC34 gene was examined to confirm the knock-out of AtUBC32, AtUBC33, and AtUBC34 in the corresponding mutants (Supplemental Figure S16C). No significant changes in morphology are observed between Col-0 and the mutants. The ubc33, ubc34, ubc32/33, ubc33/34 and ubc32/33/34 mutant plants are slightly smaller than Col-0, whereas the mutant line of *ubc32/34* is clearly smaller than that of Col-0 (Supplemental Figure S17). The ubc32, ubc33, ubc34 single, double, and triple mutant lines display slightly earlier flowering than Col-0 (Supplemental Figure S18). The AtUBC32 was shown to be required for ERAD (Cui et al., 2012b). However, whether the AtUBC33 and AtUBC34 are also required for ERAD remains unknown. We expressed the ERAD substrate MLO-12 in protoplasts derived from Col-0 and Arabidopsis *ubc32*, *ubc33*, and *ubc34* mutants and monitor the accumulation of MLO-12. Consistent with previous result (Cui et al., 2012b), the null mutation in AtUBC32 diminished the degradation of MLO-12 (Figure 5C). Like AtUBC32, loss of function in AtUBC33 and AtUBC34 also reduced the turnover of MLO-12, indicating that they are involved in ERAD as well. No synergistic effect of the ubc32, ubc33 and ubc34 mutations on the degradation of MLO-12 was observed.

### Arabidopsis UBC32, UBC33 and UBC34 Are Required for Host Immunity

The mutant lines *ubc32*, *ubc32/33*, *ubc32/34*, *ubc33/34* and *ubc32/33/34* were more susceptible than Col-0 to *Pst* strains DC3000 and DC3000Δ*hrcQ-U*, as manifested by significantly increased pathogen growth on these lines (Figure 5D and 5E). The single mutant *ubc33* and *ubc34* displayed comparable bacterial growth to that of the Col-0 whereas the double mutant *ubc33/34* displayed significantly increased bacterial growth than Col-0, indicating functional redundancy between *AtUBC33* and *AtUBC34* in host immunity. While plants of the double mutant *ubc32/33*, *ubc32/34*, and *ubc33/34* are more susceptible to pathogen infection than the single mutant *ubc32*, *ubc33*, and *ubc34*, plants of the triple mutant *ubc32/33/34* displayed comparable bacteria growth as the double mutants, implying a complex relationship beyond functional redundancy and synergy of the E2 triplet in modulating plant immunity.

## Loss of Function in Arabidopsis UBC32, UBC33 and UBC34 Do Not Change flg22

## and elf18-Triggered Seedling Growth Suppression but Alternate Plant ER Stress

### Tolerance

To elucidate the molecular underpinnings of diminished immunity in the mutant lines *ubc32*, *ubc32/33*, *ubc32/34*, *ubc33/34* and *ubc32/33/34*, we first tested whether the PRR FLS2 (Flagellin Sensing 2) and EFR (*EF*-Tu receptor)-mediated PTI are affected. FLS2 and EFR recognizes bacterial flagellin/flg22 and the elongation factor Tu/EF-Tu derived immunogenic peptide elf18, respectively to activate PTI, playing a significant role in warding off bacterial infection (Kunze et al., 2004; Zipfel et al., 2004; Yu et al., 2017). The seedling growth inhibition (SGI) assay was employed for the test, because PTI activated by flg22 and elf18 was shown to inhibit Arabidopsis seedling growth (Gómez-Gómez and Boller, 2000; Zipfel et al., 2006). As shown in Figure 6A, no significant difference in the inhibition of seedling growth was observed between the mutants and Col-0 when treated with flg22 and elf18, respectively, suggesting the FLS2 and EFR-mediated PTI was not significantly affected by loss of function in these E2 genes.

393

394

395

396

397

398

399

400

401

402

403

404

405

406

407

408

409

410

411

412

413

414

415

416

417

Consistent with the SGI assay, the FLS2 accumulation in the mutant lines was not significantly changed compared to that in Col-0, though ubc32/33 has slightly decreased whereas ubc34, ubc32/34, ubc33/34 and ubc32/33/34 display slightly increased accumulation of FLS2 (Supplemental Figure S19A). We then test whether ER stress tolerance are altered in the mutants. ER stress response has been shown to be involved in plant immunity (Moreno et al., 2012; Chakraborty et al., 2020). Indeed, both flg22 treatment and pathogen infection induce ER stress response on tomato plants, as is manifested by IRE1 (inositol-requiring enzyme 1)-mediated splicing of the ER stress response gene bZIP60 (Figure 6B and 6C). Consistent with the notion that damage to ERAD would lead to increased misfolded and unfolded proteins, the expression of the UPR marker gene Bip3 in the mutants was enhanced compared to that in Col-0 upon treatment with the ER stress agent, tunicamycin (TM) (Supplemental Figure S19B). Seedling growth assay indicated that the *ubc32* mutant displayed higher ER-stress tolerance than that of Col-0 (Figure 6D and 6E), which is consistent with previous report (Cui et al., 2012b). The ubc33 and ubc34 mutant both displayed significantly reduced tolerance to TM-induced ER stress, though the ubc33/34 double mutant did not show synergistic effect in reduction of ER stress tolerance. The ubc32/33, ubc32/34 and ubc32/33/34 displayed reduced ER-stress tolerance than Col-0, suggesting that knocking out of UBC33 and/or UBC34 in the ubc32 background suppressed the elevated ER-stress tolerance caused by the *ubc32* mutation. Similarly, transgenic N. benthamiana 32RNAi lines displayed elevated ER-stress tolerance, whereas 33/34RNAi lines displayed reduced ER-stress tolerance (Supplemental Figure S19C). These results suggest that loss of function in UBC32, UBC33 and UBC34 results in changes of plant ER stress tolerance, which likely contribute to their role in plant immunity.

#### Discussion

418

419

420

421

422

423

424

425

426

427

428

429

430

431

432

433

434

435

436

437

438

439

440

441

442

443

444

445

446

447

448

E1 enzymes govern the state of ubiquitination in an organism by coordinating the activation of ubiquitin with recruitment and charging of E2s, which in turn controls the downstream cognate E3s and substrates involved. The vital importance of E1s (and ubiquitination) for plants is demonstrated by the result that the tomato and tobacco plants died a few weeks after both E1 genes, UBA1 and UBA2 were silenced (Figure 1D, 1E and Supplemental Figure S5). Despite the importance, studies of plant ubiquitin E1s have been very limited, with essentially no functional characterizations. In the current research, we found that both tomato and N. benthamiana encode two ubiquitin E1s and the two E1s do not play equal roles in plant immunity and development, which can be attributed to differential charging of a subset of E2s by the E1 enzymes. While the two tomato E1s displayed comparable specificities to many E2s, including the groups III and IX E2s that have been previously shown to be required for plant immunity (Mural et al., 2013; Zhou et al., 2017; Zhou and Zeng, 2017), UBA2 charged E2s of group IV, V, VI, and XII with significantly higher specificities. When UBA1 is knocked down/mutated, the UBA2 can take up the duty of UBA1 to charge the E2s to which UBA1 and UBA2 possess comparable specificities. Therefore, charging of E2s in the cell is not affected and plant immunity is not compromised when UBA1 is silenced. However, when UBA2 is knocked down/mutated, charging of E2s in the group IV, V, VI, and XII is significantly reduced/abolished, which in turn will affect their cooperation with cognate E3s to ubiquitinate corresponding plant immunity-related substrates. Consequently, plant immunity is compromised when UBA2 is silenced (Figure 7). We also demonstrated that members of the group IV E2s, UBC32, UBC33, and UBC34 are required for ERAD, ER stress tolerance, and modulating of host immunity. Thus, our findings establish the connection between the E1-E2 module, ERAD, and host immunity.

Besides group IV, SIUBA2 also has much higher specificities than SIUBA1 for charging E2s in groups V, VI and XII. Conceivably, the distinct roles of the plant DUAS in plant immunity and other physiological processes, such as plant development may be attributed to differential charging of E2s in groups V, VI and XII as well. In particular, phylogenetic analysis revealed that the tomato group V E2s fall into the same subfamily

450

451

452

453

454

455

456

457

458

459

460

461

462

463

464

465

466

467

468

469

470

471

472

473

474

475

476

477

478

479

as human E2 UBE2G2 (Zhou et al., 2017). The UBE2G2 and its yeast homolog, UBC7p have been demonstrated to be involved in ERAD (Chen et al., 2006; Berner et al., 2018), which raises the possibility that the function of group V E2s are also ERAD-associated and the UBA2 of tomato and N. benthamiana and AtUBA1 of Arabidopsis play a major role in charging ER-related E2s. Characterization of the E1-E2 modules involving groups V, VI, and XII E2s will address the question and uncover their roles in different pathways. Despite being closely related phylogenetically, tomato SlUBA1 and SlUBA2 differentially charge 12 out of the 34 E2s been tested. In addition, Arabidopsis E1s AtUBA1 and AtUBA2 also differentially charge the ERAD-associated E2s AtUBC32, AtUBC33 and AtUBC34, in which Arabidopsis AtUBA1 function as the ortholog of tomato SlUBA2. Thus, Arabidopsis also possesses DUAS and differential E2 charging by the dual systems appears to be conserved in plants. It has been shown that wheat encode three ubiquitin E1s, TaUBE11, TaUBE12, and TaUBE13, but TaUBE11 and TaUBE12 are 99.2% identical in amino acid sequences (Hatfield and Vierstra, 1992), leading to the speculation that wheat also encode dual E1 activation systems for ubiquitin. Considering that nearly all sequenced crop and model plant genomes encode two or more ubiquitin Els (Supplemental Table I), plants in general likely encode dual or multiple El activation systems for ubiquitin that do not play equivalent roles in various physiological processes. In addition to intrinsic specificities in charging various E2s by the ubiquitin E1, other factors, such as PTMs that affect the activities and localizations of E1s and E2s might also contribute to the distinct roles of the plant dual E1 activation systems for ubiquitin. In mammalian cells, S-glutathionylation was reported to suppress E1 and E2 activity (Jahngen-Hodge et al., 1997). Human E1 enzyme UBE1 and E2 enzymes were found to be phosphorylated in vitro and in vivo (Kong and Chock, 1992; Cook and Chock, 1995; Stephen et al., 1996). The human Casein kinase 2 (CK2) phosphorylates E2 Cell Division Cycle 34 (CDC34) to regulate its subcellular localization (Block et al., 2001). In addition, the import and/or retention of human ubiquitin E1 UBE1 to the nucleus is cell cycle-dependent (Stephen et al., 1996). More recently, structural study of the yeast E1-E2

(UBC15) complex suggests that phosphorylation of residues at the N termini of ubiquitin E2s broadly inhibits their ability to function with ubiquitin E1 (Lv et al., 2017). Although no plant E1 and E2 enzymes for ubiquitination have been shown to be modified by other PTMs thus far, it is believed that such modifications do exist in plants (Zhang and Zeng, 2020), which may serve as an extra layer of modulation in addition to differential E2 charging that lead to distinct roles of the plant DUAS.

480

481

482

483

484

485

486

487

488

489

490

491

492

493

494

495

496

497

498

499

500

501

502

503

504

505

506

507

508

509

510

Our findings indicate that the UBC32, UBC33 and UBC34 E2 triplet function in ERAD and plant immunity, which is conserved in tomato, tobacco and Arabidopsis. Thus, in addition to abiotic stress (Cui et al., 2012b; Ahn et al., 2018), UBC32, UBC33 and UBC34 also function in biotic stresses. The null mutants for UBC32, UBC33, and UBC34 do not display significant morphological changes, which suggest that alterations of host immunity in the mutants are unlikely caused by changes in growth and development and their role in abiotic and biotic stress pathways are specific. Noteworthy, although the enhanced bacterial growth in UBC32 knocking-out Arabidopsis mutant ubc32 and tobacco knocking-down UBC32i plants was significant compared to the control plants, the enhanced level of pathogen growth in ubc32 and UBC32i plants is always lower than that of the Arabidopsis ubc33/ubc34 mutant plants and the tobacco UBC33/34i plants, respectively (Figure 3F, 5D and 5E), suggesting that UBC33 and UBC34 together contribute more to plant immunity than UBC32. The diminished plant immunity in the ubc33/ubc34 mutant plants is in line with the result that the ubc33 and ubc34 mutant display reduced ER stress tolerance, as ER stress tolerance have been shown to be required for plant immunity (Wang et al., 2005; Moreno et al., 2012). By contrast, the *ubc32* mutant displays diminished immunity yet elevated ER stress tolerance, which suggests ER stress tolerance is not the sole factor that contribute to the role of UBC32 in host immunity. Indeed, previous reports indicated that UBC32 as an ERAD component negatively modulate ER stress tolerance, salt tolerance yet positively regulate oxidative burst tolerance (Cui et al., 2012a; Cui et al., 2012b). It is conceivable that the UBC32, UBC33 and UBC34 E2s can function in ERAD to target substrates of different pathways and the combination of UBC32, UBC33, and UBC34 actions at ER determine the outcome of the E2 triplet mediated ERAD in modulating plant immunity. Our results

demonstrated that loss of function in the E2 triplet do not significantly affect FLS2 and EFR-mediated immunity, suggesting FLS2 and EFR may not be a key target of the E2triplet-mediated ERAD in the modulation of host immunity. Previous studies showed that loss of function in the ER protein folding-related genes significantly affect biogenesis of EFR, whereas have merely marginal effect on that of FLS2 (Li et al., 2009; Nekrasov et al., 2009; Saijo et al., 2009). Thus, the ER apparently facilitates the folding but not degradation in the biogenesis of EFR. There are usually dozens of E2s and hundreds of E3s in a given plant genome (Vierstra, 2003; Zhou et al., 2017). Conceivably, loss of function in UBC32, UBC33 and UBC34 E2 triplet is believed to affect their cooperation with multiple cognate E3s and consequently, the modification of many substrates that reside in various pathways. It is possible that the E1-UBC32/33/34 E2 triplet module work with different E3s to modify different substrates that reside in abiotic and biotic stress pathway, respectively. In this regard, uncover and characterization of the cognate E3s and key substrates of the UBC32/33/34 E2 triplet mediated ERAD and ER stress signaling in the context of plant immunity would be the key to an in-depth understanding of the regulation of host immunity by ERAD.

#### **Materials and Methods**

#### **Growth of Bacteria and Plant Materials**

Agrobacterium tumefaciens strains GV3101 and GV2260 and strains of *Pseudomonas* syringae pv tomato (*Pst*) and *Pseudomonas fluorescens* 55 were grown at 28°C on Luria-Bertani and King's B medium, respectively, with appropriate antibiotics. *N. benthamiana* and tomato RG-pto11 (*pto11/pto11*, *Prf/Prf*) seeds were germinated and plants were grown on autoclaved soil in a growth chamber with 16 h light (~ 300 μmol/m²/s at the leaf surface of the plants), 24°C/23°C day/night temperature, and 50% relative humidity. Arabidopsis mutant lines SALK\_082711 (*ubc32*) (Cui et al., 2012b), SALK\_104882C (*ubc33*) and CS878883 (*ubc34*) (Ahn et al., 2018) were obtained from ABRC. All Arabidopsis plants were grown in a growth chamber with 16 h light (~ 300 μmol/m²/s at the leaf surface of the plants), 22°C/22°C day/night temperature, and 50% relative humidity.

### **DNA Manipulations and Plasmid Constructions**

542

545

546

556

557

566

567

- 543 All DNA manipulations were performed using standard techniques (Sambrook and
- Russell, 2001). A detailed methodology is described in Supplemental Methods S1.

### **Sequence Alignment and Phylogenetic Analysis**

- For sequence alignment, sequences of interest in the FASTA format were entered into the
- ClustalX 2.1 program and aligned using the ClustalX algorithm (Larkin et al., 2007). The
- 549 phylogenetic analysis was then performed with the MEGAX program using the aligned
- sequences (Tamura et al., 2013). To build an unrooted phylogenetic tree using MEGAX,
- 551 the evolutionary history was inferred using the neighbor-joining method with 1000
- bootstrap trials. The evolutionary distances were computed using the p-distance method
- 553 in which the evolutionary distance unit represents the number of amino acid (or
- nucleotide) substitutions per site (Nei and Kumar, 2000). Branches corresponding to
- partitions reproduced <50% bootstrap replicates were collapsed in the tree.

### **Expression and Purification of Recombinant Proteins**

- 558 GST-tagged fusion proteins were expressed in E. coli strain BL21 (DE3) and purified
- with Glutathione Sepharose 4 Fast Flow beads (GE Healthcare) by following the protocol
- 560 provided by the manufacturer. The purified proteins were further desalted and
- concentrated in the protein storage buffer (50 mM Tris-HCl pH8.0, 50 mM KCl, 0.1 mM
- EDTA, 1 mM DTT, 0.5 mM PMSF) using the Amicon Centrifugal Filter (Millipore). The
- desalted and concentrated recombinant protein was stored at -80 °C in the presence of a
- 564 final concentration of 40% glycerol until being used. The concentration of purified
- protein was determined using protein assay agent (Bio-Rad).

#### Examination of Charging Ubiquitin E2s by E1s via Thioester Assay

- To examine the efficiencies of charging E2s by E1s, the thioester assay was performed as
- described with modifications (Mural et al., 2013). In a 15 µL reaction, 40 ng of ubiquitin
- 570 E1 (tomato E1 GST-SlUBA1, GST-SlUBA2, tomato chimeric E1 GST-SlUBA1-
- 571 Ufd<sup>SIUBA2</sup>, GST-SIUBA2-Ufd<sup>SIUBA1</sup>, Arabidopsis GST-AtUBA1, and GST-ATUBA2,
- respectively) was pre-incubated with 2.0 µg of FLAG-ubiquitin in 20 mM Tris-HCl pH

7.5, 10 mM MgCl<sub>2</sub>, and 1 mM ATP at 28 °C for 10 min, which is followed by adding 100 ng of the GST or 6HIS - fused E2 protein to be tested. The reaction was then continued for 15 min before being stopped with SDS sample loading buffer (62.5 mM Tris-HCl pH 6.8, 2% SDS, 0.01% bromophenol blue, 10% glycerol and 4M Urea). To test the DTT sensitivity of E2-ubiquitin linkage in the thioester assay, the reaction volume was scaled up to 20 µL. The reaction was then equally split and terminated by addition of SDS sample loading buffer with either 100 mM dithiothreitol (DTT+) or 4 M urea sample buffer (DTT-). The reactions were immunoblotted with mouse monoclonal anti-FLAG M2-peroxidase-conjugated antibody (Sigma-Aldrich) before being detected using ECL kit (Pierce, now Thermo Fisher). The formation of DTT-sensitive ubiquitin adducts to tomato E2 SlUBC3 is denoted as charged E2. 

### **Quantitative real time-PCR (qRT-PCR)**

For detecting gene expression, samples of tomato root, stem, leaf, sepal, petal, ovary and green fruit from 10-week-old tomato plants; Leaf tissues of 3 to 4-week old tomato RG-pto11 (pto11/pto11, Prf/Prf) plants infiltrated with 2 μM flg22 or sterilized H<sub>2</sub>O (mock, used as control); leaf tissues of tobacco E2-RNAi transgenic lines and VIGS plants; and leaf tissues from Arabidopsis plants with different treatments were collected for total RNA extraction using the RNeasy Plant Mini Kit with DNase treatment (QIAGEN) by following the protocol provided by the manufacturer. The first-strand cDNA was synthesized using the Superscript III reverse transcriptase and oligo dT primer (Life Technologies) according to the instructions from the manufacturer. Quantitative real-time PCR (qRT-PCR) was performed using gene specific primers and SYBR Green (Life Technologies) on the LightCycler® 480 Instrument II (Roche). All primers used in qRT-PCR are showed in the Supplemental Table III. SIEF1a, NbEF1a and AtActin2 were used as the internal references for tomato, N. benthamiana and Arabidopsis samples, respectively.

#### Yeast Two-Hybrid

For testing the interaction of two proteins using the LexA-based yeast two-hybrid system, procedures were followed as described (Golemis et al., 2008). For detecting interaction of

- HRD1A, HRD1B and HRD3A with UBC32, UBC33 and UBC34 using the mating-based
- split-ubiquitin system (mbSUS), the experiment was performed as described (Grefen et
- al., 2009). A detailed methodology is described in Supplemental Methods S1.

### Bimolecular fluorescence complementation (BiFC) Assay

- The BiFC assay that is based on split yellow fluorescent protein (YFP) was used to test
- 610 the interaction of various E1-E1, E1-E2, and E2-E3 pairs in the leaves and protoplasts by
- following the protocol as described (Zhou et al., 2017). A detailed methodology is
- described in Supplemental Methods S1.

### Coimmunoprecipitation

607

608

613

614

618

619

- 615 The coimmunoprecipitation assay of HA-tagged E1s and FLAG-tagged E2s was
- performed as described previously (Zhou et al., 2017). A detailed methodology is
- described in Supplemental Methods S1.

### Seedling growth assay

- To test FLS2 and EFR-mediated immunity in Arabidopsis ubc32, ubc33, and ubc34
- single, double and triple mutant lines, seedling growth inhibition assay was performed as
- described (Wierzba and Tax, 2016). Specifically, Arabidopsis seeds were sterilized and
- then sowed on ½ MS (Murashige and Skoog) agar plates for stratification for 3 days,
- followed by moving the plates to short day conditions (22 °C, 10 h light, and 65-70%)
- 625 relative humidity) for germination for 3 days. The seedlings of Col-0 and different
- mutants were then transferred to liquid or solid (by adding agar) ½ MS media with or
- without 100 nM flg22 or 25 nM elf18 for 7 days before photographing. To detect the ER-
- stress tolerance of different Arabidopsis mutant lines and tobacco RNAi transgenic lines,
- 629 sterilized Arabidopsis and tobacco seeds were scattered in the ½ MS plate with
- tunicamycin (Tm) at 0.025 (for Arabidopsis seeds) or 0.03 (for tobacco seeds) µg/mL.
- The development of Arabidopsis and tobacco seedlings was observed and photographed
- one or two weeks after sowing. Four kinds of leaf phenotypes (Green, light green, light
- 633 yellow and yellow) for Arabidopsis seedlings and three kinds of leaf phenotypes (Green,

- light yellow and yellow) for tobacco seedlings were statistically calculated for the relative
- 635 ER-stress tolerance.

636

637

#### **Virus-Induced Gene Silencing (VIGS)**

- 638 Gene silencing was induced using the tobacco rattle virus (TRV) vectors (Caplan and
- Dinesh-Kumar, 2006) as previously described (Mural et al., 2013). Agrobacterium
- (OD600 = 0.5) containing appropriate pTRV plasmids was induced with acetosyringone
- and used to infiltrate two leaf-stage tomato seedlings and 3-week-old N. benthamiana
- seedlings. VIGS-treated tomato plants were maintained for 3 to 4 weeks at 21°C /21°C,
- 643 16/8 h day/night condition, whereas VIGS-treated N. benthamiana plants were
- maintained for 3 to 4 weeks at 24°C /22°C, 16/8 h day/night condition to allow silencing
- 645 to occur.

646

647

658

659

### **Extraction of Plant Total Proteins and Immuno-blotting**

- Each tomato and tobacco sample was homogenized in 300 μl 1× Laemmli buffer and
- 649 then boiled for 5 min, followed by being resolved using 10% SDS-PAGE. Each
- 650 Arabidopsis sample was homogenized in 300 μl protein extraction buffer (25 mM Tris-
- 651 HCl, pH 7.5, 150 mM NaCl, 5% glycerol, 0.05% Nonidet P-40, 2.5 mM EDTA, 1 mM
- 652 phenylmethylsulfonyl fluoride and 1× complete cocktail of protease inhibitors). The
- 653 concentration of total proteins was determined using protein assay agent (Bio-Rad).
- 654 Extraction of each sample containing 20 μg proteins was added with 2× SDS protein
- loading buffer and boiled for 5 min, then resolved by 10% SDS-PAGE. The immuno-
- 656 blottings were performed with appropriate antibodies: anti-FLAG (Sigma), anti-HA
- 657 (Sigma), anti-MYC (Santa Cruz), and anti-Ub (P4D1) (Santa Cruz).

#### **Bacterial Population Assay**

- The bacterial population assay was conducted as described previously (Katagiri et al.,
- 661 2002; Nguyen et al., 2010). Briefly, for assaying the DC3000 $\Delta hopQ1$ -1 growth, N.
- benthamiana plants about four weeks after VIGS infection were first vacuum infiltrated
- with P. fluorescens 55 (P. flu55) by submersion of the aerial parts of the plant in a
- suspension of P. flu55 (5  $\times$  10<sup>7</sup> CFU/mL) containing 0.002% Silwet L-77 and 10 mM

MgCl<sub>2</sub>. The plants were then inoculated with Pst DC3000 $\Delta$ hopO1-1 (2 × 10<sup>5</sup> CFU/mL) in 665 the presence of 0.002% Silwet L-77 and 10 mM MgCl<sub>2</sub> by vacuum infiltration 7 h after 666 667 the treatment with P. flu55. For assaying the growth of Pst strains DC3000 and DC3000\(\textit{LhrcQ-U}\), about four-week-old Arabidopsis or tomato plants about four weeks 668 after VIGS infection were inoculated with the suspension of pathogen DC3000 (1  $\times$  10<sup>6</sup> 669 CFU/mL) and DC3000\(Delta hrcO-U\) (1 \times 10^9 CFU/mL) containing 0.002\% Silwet L-77 and 670 671 10 mM MgCl<sub>2</sub> by vacuum infiltration. In addition, the dipping method was also used for inoculation of tomato plants with DC3000\(Delta hrcQ\)-U (1 \times 10^9 CFU/mL). Inoculated plants 672 were maintained in a growth chamber and monitored daily for symptom development. To 673 assess bacterial populations, leaf discs were harvested from three to four plants of each 674 675 treatment on day 3 and day 4 after the inoculation and ground, serially diluted, and plated to determine the amount of the bacteria grown as described (Zhou et al., 2017). 676

### **Cell Death Suppression Assay**

677

678

687

688

- The cell death suppression assay was performed as previously described (Nguyen et al.,
- 680 2010). The *P. fluorescens* 55 at the concentration of  $OD_{600}$  equal to 0.5 (~ 2.5 × 10<sup>8</sup>
- 681 CFU/mL), 0.1 ( $\sim 5 \times 10^7$  CFU/mL), and 0.015 ( $\sim 7.5 \times 10^6$  CFU/mL), respectively were
- used as the PTI inducer. The *Pst* strain DC3000 at the concentration of  $2 \times 10^6$  CFU/mL
- was used as the challenger in the assay. The challenge of PTI was conducted 7h after PTI
- 684 induction. Appearance of cell death in the overlapping area, where both the inducer and
- challenger were infiltrated was assessed. Photographs were taken on the fourth day after
- 686 infiltration of *Pst* DC3000.

### **Accession Numbers**

- 689 Sequence data of tomato, Arabidopsis, N. tabacum, N. benthamiana, wheat and soybean
- 690 that were used in this article can be found in the GenBank data library based on the
- 691 accession numbers: SlUBA1, Solyc06g007320.2.1; SlUBA2, Solyc09g018450.2.1;
- 692 NbUBA1 Niben101Scf09017g00015.1; NbUBA2, Niben101Scf03202g13010.1;
- 693 GmUBA3 (Glyma.02G229700), XP 003518319; GmUBA2 (Glyma.11G166100),
- 694 XP 006591250; GmUBA1 (Glyma.14G196800), KRH17078; GmUBA4
- 695 (Glyma.18G058900), XP 006602078; TaUBE11, P20973.1; TaUBE12, P31251.1;

- 696 TaUBE13, P31252.1; AtUBA1, AT2G30110; AtUBA2, AT5G06460; AtUBC32,
- 697 AT3G17000; AtUBC33, AT5G50430; AtUBC34, AT1G17280; SIUBC32, KY246924;
- 698 SIUBC33, KY246925; SIUBC34, KY246926; SIHRD1A, Solyc03g096930.2.1;
- 699 SIHRD1B, Solyc06g072790.2; SIHRD3A, Solyc03g118670.2.

#### Acknowledgments

700

701

710

711

- We thank Christian Elowsky and You Zhou (Biotechnology Center, University of
- Nebraska-Lincoln) for helping with the confocal microscope and G.B. Martin for critical
- reading of the manuscript. We are grateful to Harkamal Walia for sharing the barley
- seeds for cloning of the MLO gene. We also thank the *Arabidopsis* Biological Resource
- 706 Center for the *Arabidopsis* T-DNA insertion lines. This work was supported by start-up
- funds from the University of Nebraska-Lincoln, the U.S. Department of Agriculture
- National Institute of Food and Agriculture (grant no. 2012-67014-19449), and the
- National Science Foundation (grant no. IOS-1645659) to L.Z.

#### **Author Contribution**

- 712 B.Z. designed experiments, performed most experiments, analyzed data, and wrote the
- 713 manuscript. X. C. cloned the two tomato E1 genes, purified recombinant E1 and some E2
- 714 proteins and conducted the thioester assay to measure specificities of the tomato E1s in
- charging some E2 enzymes. C.W. examined the accumulation of MLO-12 in N.
- benthamiana UBC32i and UBC33/34i transgenic lines and the Arabidopsis ubc32, ubc33,
- and ubc34 single, double and triple mutants, and performed the flg22 and elf18-triggered
- seedling growth inhibition assay. Y. Z. examined the subcellular localization of tomato
- 719 SIHRD1A and SIHRD1B. L.Z. designed experiments, analyzed the data, and edited the
- 720 manuscript.

721

722

723

### Figure Legends

- Figure 1. Tomato genome encodes two ubiquitin E1s that function differentially in
- 725 plant development and host immunity. (A) The tomato proteins SIUBA1 and SIUBA2
- encode active E1 enzyme. The numbers on the right denote the molecular mass of marker

728

729

730

731

732

733

734

735

736

737

738

739

740

741

742

743

744

745

746

747

748

749

750

751

752

756

757

proteins in kD. The experiment was repeated two times with similar results. (B) The SlUBA1 and SlUBA2 genes show comparable level of expression in various tomato organs. (C) SIUBA1 and SIUBA2 are presented in both cytoplasm and nucleus. GFPfused SIUBA1 and SIUBA2 in tobacco leaves was examined by confocal microscopy. Bars =  $20 \mu m$ . (D) and (E) The tomato and tobacco E1s differentially regulate plant development. Tomato (**D**) and tobacco (**E**) plants in which the E1 gene UBA1 (TRV-UBA1), UBA2 (TRV-UBA2) or both (TRV-UBA1/2) are silenced are shown. The nonsilenced TRV empty vector (TRV) was used as control. Up panel: side view; low panel: top view. Photographs were taken 4 weeks after the approximately 3-week-old seedlings were infiltrated with corresponding VIGS construct. (F) VIGS of UBA2 gene in N. benthamiana compromised PTI-mediated cell death suppression. Black dashed circles denote the infiltration area of P. fluorescens 55 (P. flu55) while white dashed circles denote infilatration area of Pst strain DC3000. Numbers at the left side denote the corresponding concentration of P. flu55 (OD<sub>600</sub> value) used to activate PTI. Numbers at the right side of each image represent the number of overlapped infiltration areas that displayed cell death and the total number of infiltrated overlapping areas. Photographs were taken on day 4 after infiltration of Pst DC3000. Bar = 1 cm. (G) and (H) Bacterial growth on the UBA1- and UBA2-silenced tomato (G) and tobacco (N. benthamiana) (H) plants. Non-silenced (TRV) plants were used as control. Tomato VIGS Plants (G) were vacuum infiltrated with Pst strain DC3000∆hrcO-U. Tobacco VIGS Plants (H) were vacuum infiltrated with P. flu55 to induce PTI and then inoculated with Pst strain DC3000\(Delta\)hopO1-1 six hours later. Experiments were repeated three times with similar results. Asterisks indicate significantly elevated bacterial growth compared to the control plants based on the one-way ANOVA (P < 0.01).

### Figure 2. The tomato E1s display different specificities to E2s in vitro and in vivo. (A)

SIUBA1 and SIUBA2 differentially charge groups IV (SIUBC32, 33 and 34) and V (SIUBC7, 14, 35 and 36) E2s in thioester assay. The experiment was repeated at least three times with similar result. SIUBC3 was used as control. (B) SIUBA1-Ufd<sup>SIUBA2</sup> and

SlUBA2-Ufd<sup>SlUBA1</sup> reverse the specificities of SlUBA1 and SlUBA2 in charging group

IV and V E2s. The numbers on the right denote the molecular mass of marker proteins in

kilodaltons. Experiments were repeated three times with similar results. (C) The interaction of SIUBA1 and SIUBA2 with group IV E2s was detected by yeast two-hybrid. SIUBC8 and the empty prey and bait vectors (EV) were used as control. Interaction was demonstrated by activation of the lacZ reporter gene (blue patches). Photographs were taken 24 h after streaking the yeast cells onto plates containing X-Gal. The low left panel shows ratio of blue color intensity in yeast cell patches of UBA1-E2 compared to that of the UBA2-E2 as shown in upper left panel. The right panel shows comparable level of SIUBA1 and SIUBA2 protein and similar level of the E2 protein were expressed for each pair of SIUBA1-E2 and SIUBA2-E2 in the yeast cells. CBS, Coomassie blue staining as an indicator of equal sample loading. (D) Tomato UBA2 showed significantly stronger interaction with SIUBC32, SIUBC33 and SIUBC34 than UBA1 in the BiFC assay. SIUBC12 was used as control. Images from four random microscopic fields for each tested construct pair were presented. The experiment was repeated two times with similar results. Scale bar = 20 um. Low panel shows the level of protein expressed in planta for the E1 (UBA1 or UBA2)-E2 pairs tested in the assay. (E) and (F) Significantly higher amount of tomato UBA2 than UBA1 was pulled down by SIUBC32, SIUBC33 and SlUBC34 in co-immunoprecipitation assay. FLAG-tagged SlUBC12 and GFP were used as negative controls. The experiment was repeated two times with similar result.

Figure 3. Group IV E2s are required for plant immunity. (A) and (B) The expression of tomato SIUBC32, 33 and 34 genes was induced by flg22 (A) and different Pst strains (B). The expression of SIUBC32, SIUBC33 and SIUBC34 were analyzed by qRT-PCR using tomato  $EF1\alpha$  gene as the internal reference. The experiment was performed with three technical repeats in each of the three biological replicates. Error bars indicate standard deviation. Asterisks indicate significantly elevated expression compared to mock plants at the same time point based on the one-way ANOVA (P < 0.01). (C) and (E) The E2 genes were efficiently and specifically silenced in tomato (C) and tobacco (E) plants. The accumulation of the transcript for E2 genes was quantified by qRT-PCR.  $EF1\alpha$  was used as an internal reference. In tomato (C), plants infected with the empty TRV vector were used as control (TRV). In tobacco (E), wild type plants were used as control. The relative quantity of transcript for corresponding gene in control plants was

790

791

792

793

794

795

796

797

798

799

800

801

802

803

804

805

806

807

808

809

810

811

812

813

814

815

816

817

818

819

set as 1. Experiments were repeated at least two times with similar results. (**D**) Knocking down the expression of tomato group IV E2 genes significantly increased bacterial growth (DC3000 $\Delta hrcQ$ -U) compared to the control plants infected with the TRV empty vector (TRV). The dipping method was used for pathogen inoculation. (**F**) Knocking down the expression of tobacco group IV E2 genes in transgenic plants significantly increased bacterial growth (DC3000 $\Delta hopQI$ -I) compared to the control plants. In (**D**) and (**F**), asterisks indicate significantly increased bacterial growth compared to control plants based on the one-way ANOVA (P < 0.01).

Figure 4. Tomato UBC32, UBC33, and UBC34 are endoplasmic reticulum (ER)bound and are involved in ERAD. (A) Tomato E2s SlUBC32, SlUBC33 and SlUBC34 are localized to the ER. GFP-fused wild type and transmembrane domain-deleted ( $\Delta$ TMD) mutant version of SlUBC32, SlUBC33 and SlUBC34 were examined using confocal microscope. GF, green fluorescence; RF, red fluorescence conferred by mCherry-ER-localized marker protein (ER-rb). (B) SIUBC32, SIUBC33 and SIUBC34 interacted with tomato homolog of ERAD-associated ubiquitin E3 ligases, SlHRD1A and SIHRD1B and their adapter protein SIHRD3A in the mating-based split ubiquitin yeast two-hybrid system. Growth of yeast cells harboring two genes that had been fused with the N-terminal (Nub) and C-terminal (Cub) halves of the ubiquitin protein, respectively on SC-ADE+HIS+, SC- and SC- with 0.15 M MET media plates, respectively, were shown in the left, middle and right panel. Empty bait and prey vector (EV) were used as control. (C) SIUBC32, SIUBC33 and SIUBC34 interacted with SIHRD1A and SIHRD1B in BiFC assay using tomato leaf protoplasts. EV, empty vector; FL., fluorescence; Chl., chlorophyll autofluorescence; Bright, bright field image. Scale bar = 20 µm. (D) Transient co-expression in N. benthamiana leaves of the group IV E2 and the known ERAD target MLO-12 increased degradation of MLO-12. GFP was used as control. (E) Knocking down UBA2 and group IV E2s in leaves of N. benthamiana plants by VIGS reduced the degradation of MLO-12. (F) Degradation of MLO-12 was reduced in N. benthamiana RNAi transgenic lines where group IV E2 genes was silenced. Two independent transgenic lines in which the NbUBC32 gene and the NbUBC33 and NbUBC34 genes were silenced, respectively were used for the assay. The experiments in

821

822

823

824

825

826

827

828

829

830

831

832

833

834

835

836

837

838

839

840

841

842

843

844

845

846

847

848

849

850

(E) and (F) were repeated two times with similar result. In (D), (E) and (F), the FLAGtagged GFP was expressed together with HA-tagged MLO-12 as an internal control of efficiency in transient expression as well as control of non-misfolded protein. Staining of the Rubisco large subunit (Rubisco) by Coomassie Blue R250 denotes equal sample loading. Figure 5. Arabidopsis E2 enzymes AtUBC32, AtUBC33 and AtUBC34 are differentially charged by the E1s AtUBA1 and AtUBA2 and are required for ERAD and host immunity. (A) Tomato SlUBC32 was charged by AtUBA1 with higher specificities than that of AtUBA2 in thioester assay. The tomato SlUBC12 to which tomato E1 display comparable specificities was used as control. (B) The Arabidopsis E2s AtUBC32, AtUBC33 and AtUBC34 were charged by AtUBA1 at significantly higher efficiencies than that of AtUBA2 in thioester assay. The AtUBC8 was used as control. The experiments in (A) and (B) were repeated two times with similar result. (C) Loss of function in AtUBC32, AtUBC33 and AtUBC34 diminished the degradation of MLO-12 by ERAD. MLO-12 was transiently expressed in protoplasts derived from leaves of Col-0 and the mutants, respectively. The GFP-HA was used as internal control for transfection efficiencies. (D) and (E) Bacterial growth assay on single, double and triple mutants of the Arabidopsis mutant ubc32, ubc33 and ubc34. Wild-type Col-0 and different mutants for the AtUBC32, AtUBC33 and AtUBC34 gene were infected with DC3000 (D) and DC3000\(\textit{ArcQ-U}\) (E), and then the bacterial population was examined on 2 and 3 days after infection. Bars show standard deviation. Asterisks indicate significantly elevated bacterial growth compared with the WT plants based on one-way ANOVA (P < 0.01). cfu, colony-forming units. The experiments were repeated three times with similar results. Figure 6. Knocking out AtUBC32, AtUBC33, and At UBC34 do not affect flg22 and elf18-triggered seedling growth inhibition but alternate plant ER stress tolerance. (A) Phenotype of wild-type Col-0 and ubc32, ubc33, ubc34 single, double, and triple mutant seedlings untreated or treated with flg22 and elf18. The fls2 and efr mutant were

included as control. Similar results were obtained in three independent experiments. (B)

and (C) ER stress response is involved in plant immunity. Quantitative measurement of

29

bZIP60 mRNA splicing activity was performed by qRT-PCR analyses of spliced (bzip60S) and non-spliced (bzip60U) bZIP60 forms. Ratios of bzip60S to bzip60U are calculated, with setting the ratio of uninfected Col-0 as 1. (**B**) qRT-PCR analyses of bzip60S and bzip60U in 10-day tomato seedlings with 1  $\mu$ M flg22 treatment in ½ liquid MS media were conducted. Ratios of spliced bzip60S and unspliced bzip60U was shown. (**C**) Ratios of spliced bzip60S and unspliced bzip60U was shown for 3-week tomato plants infected with *Pst* pathogens by dipping method. Statistical analysis was performed using Student's t-test. \*, p≤0.05. \*\*, p≤0.001. The experiments were performed at least two times with similar results. (**D**) and (**E**) The phenotypes of different Arabidopsis *ubc32*, *ubc33* and *ubc34* mutant lines grew on media without (**D**) or with 0.025  $\mu$ g/mL tunicamycin (**E**) in seedling growth assay. The percentages of different phenotypes are shown in the right panels. A representative image of two independent experiments is shown. For quantification of seedling phenotypes, n ≥ 30 (right panel). Bar = 0.5 cm. Photos were taken 7 days after sowing cold stratification-processed seeds on the growth media.

Figure 7. A working model illustrates how the plant DUAS function distinctly in host immunity. The two tomato E1s display comparable specificities to E2s of groups I, II, III, VIII, IX and X. However, UBA2 charges E2s of groups IV, V, VI, and XII with significantly higher specificities, which contribute to the distinct roles of UBA1 and UBA2 in plant growth, development, and defense. In the absence of UBA1, UBA2 can charge the E2s of group I, II, III, VIII, IX and X efficiently and the charging of groups IV, V, VI, and XII E2s is also not affected. By contrast, knocking out UBA2 will significantly reduce the charging of group IV, V, VI, and XII E2s, which in turn will affect cooperation of them with cognate E3s, such as working with ERAD-related E3s by group IV E2s, to modulate cognate plant immunity-related substrates by ubiquitin. Consequently, plant immunity is diminished. Nearly all sequenced plant genomes encode two or more ubiquitin E1s. Thus, plants likely encode dual or multiple E1 activation systems for ubiquitin that do not play equivalent roles in various physiological processes. Fonts in red color denotes that group III, IV, and IX E2s have been shown to modulate plant immunity. The question mark indicates that the role of group V, VI and XII E2s in

plant immunity is unclear. Ub, ubiquitin; NLR, nucleotide-binding leucine-rich repeat

protein; Pst, Pseudomonas syringae pv. tomato.

882

883

884

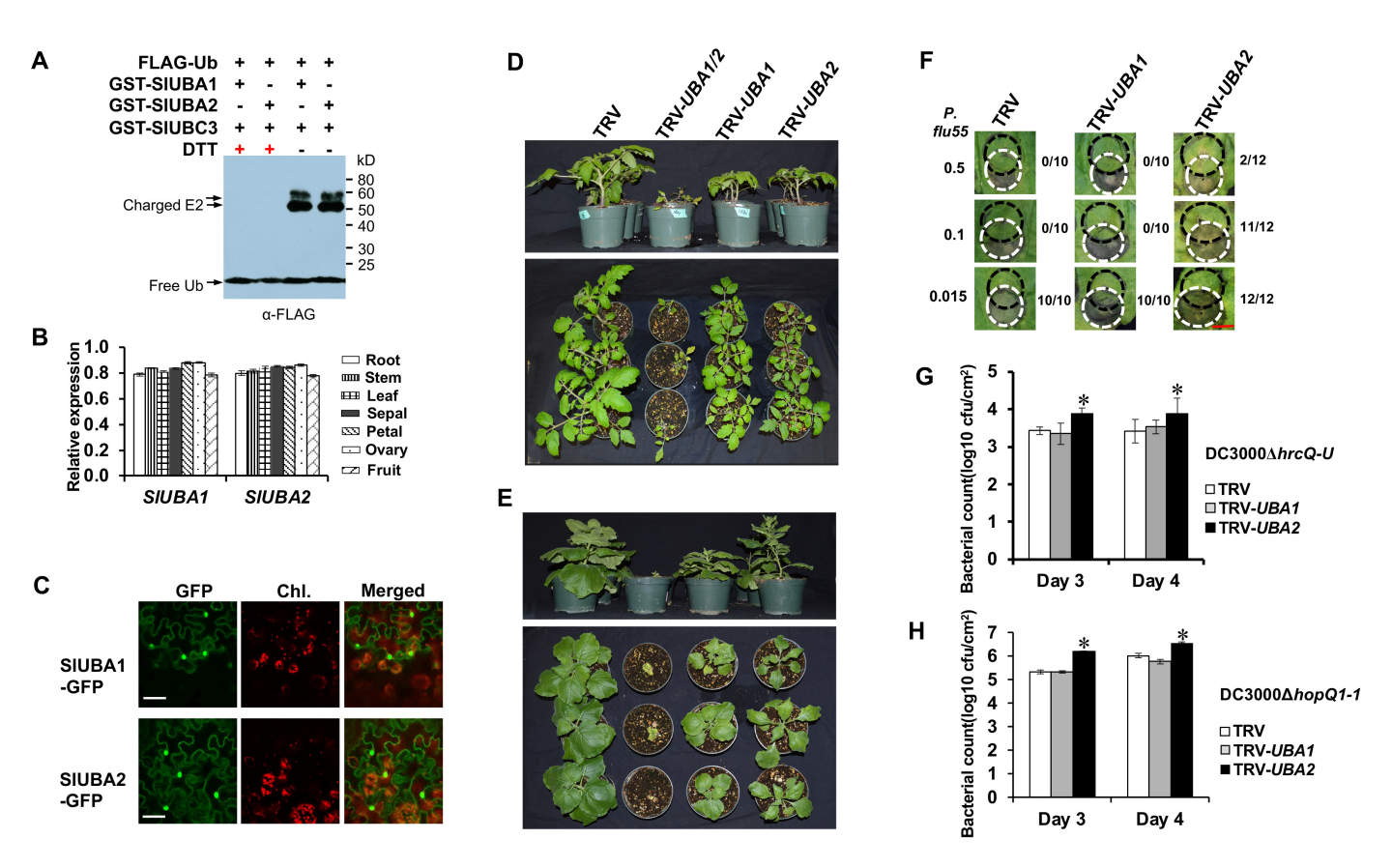


Figure 1. Tomato genome encodes two ubiquitin E1s that function differentially in plant development and host immunity. (A) The tomato proteins SIUBA1 and SIUBA2 encode active E1 enzyme. The numbers on the right denote the molecular mass of marker proteins in kD. The experiment was repeated two times with similar results. (B) The SIUBA1 and SIUBA2 genes show comparable level of expression in various tomato organs. (C) SIUBA1 and SIUBA2 are presented in both cytoplasm and nucleus. GFP-fused SIUBA1 and SIUBA2 in tobacco leaves was examined by confocal microscopy. Bars =  $20 \mu m$ . (D) and (E) The tomato and tobacco E1s differentially regulate plant development. Tomato (D) and tobacco (E) plants in which the E1 gene UBA1 (TRV-UBA1), UBA2 (TRV-UBA2) or both (TRV-UBA1/2) are silenced are shown. The non-silenced TRV empty vector (TRV) was used as control. Up panel: side view; low panel: top view. Photographs were taken 4 weeks after the approximately 3-week-old seedlings were infiltrated with corresponding VIGS construct. (F) VIGS of UBA2 gene in N. benthamiana compromised PTI-mediated cell death suppression. Black dashed circles denote the infiltration area of P. fluorescens 55 (P. flu55) while white dashed circles denote infilatration area of Pst strain DC3000. Numbers at the left side denote the corresponding concentration of P. flu55 (OD<sub>600</sub> value) used to activate PTI. Numbers at the right side of each image represent the number of overlapped infiltration areas that displayed cell death and the total number of infiltrated overlapping areas. Photographs were taken on day 4 after infiltration of Pst DC3000. Bar = 1 cm. (G) and (H) Bacterial growth on the UBA1- and UBA2-silenced tomato (G) and tobacco (N. benthamiana) (H) plants. Non-silenced (TRV) plants were used as control. Tomato VIGS Plants (G) were vacuum infiltrated with Pst strain DC3000∆hrcQ-U. Tobacco VIGS Plants (H) were vacuum infiltrated with P. flu55 to induce PTI and then inoculated with Pst strain DC3000\(\textit{AhopQ1-1}\) six hours later. Experiments were repeated three times with similar results. Asterisks indicate significantly elevated bacterial growth compared to the control plants based on the one-way ANOVA (P < 0.01).

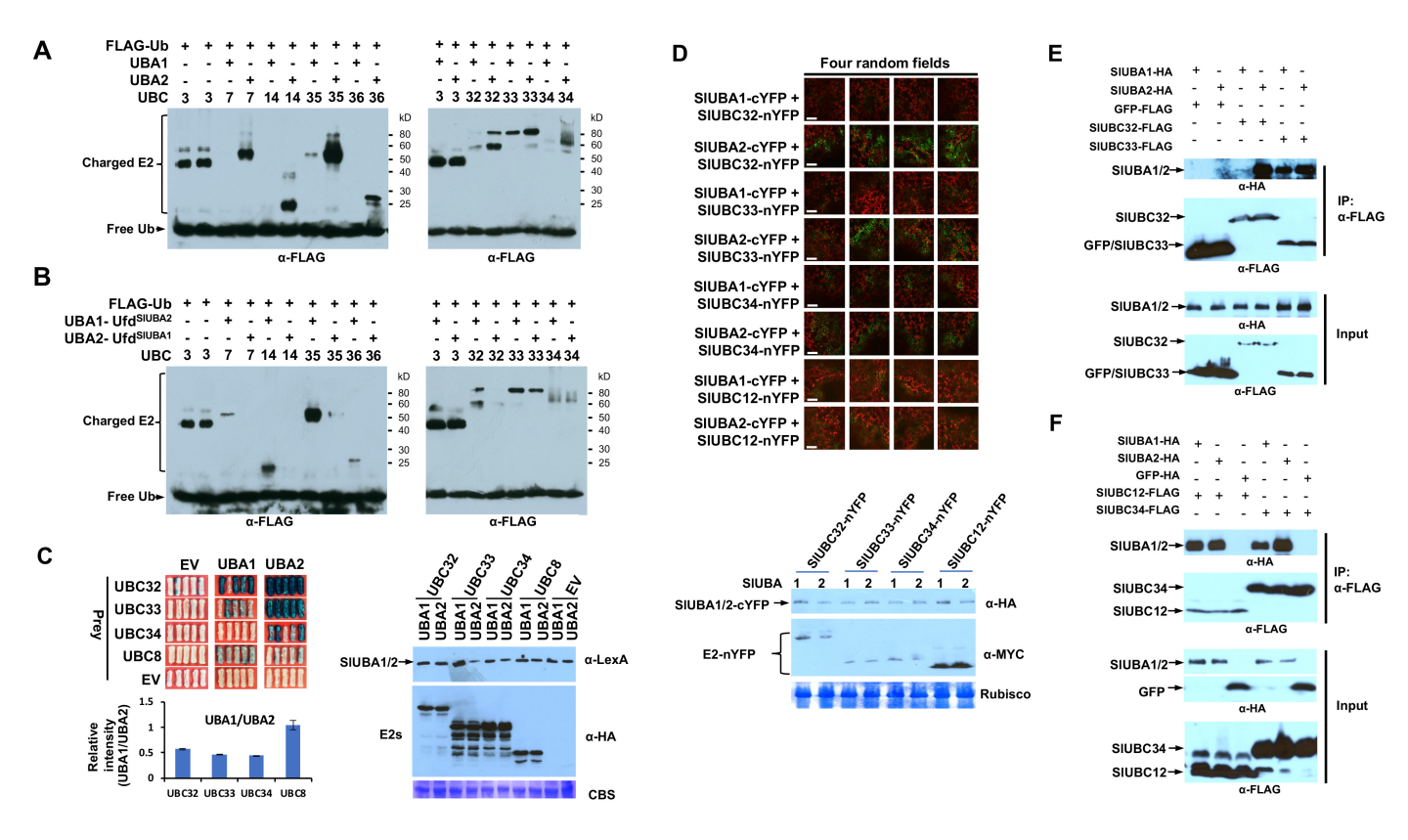


Figure 2. The tomato E1s display different specificities to E2s in vitro and in vivo. (A) SIUBA1 and SIUBA2 differentially charge groups IV (SIUBC32, 33 and 34) and V (SIUBC7, 14, 35 and 36) E2s in thioester assay. The experiment was repeated at least three times with similar result. SlUBC3 was used as control. (B) SlUBA1-UfdSlUBA2 and SlUBA2-UfdSlUBA1 reverse the specificities of SIUBA1 and SIUBA2 in charging group IV and V E2s. The numbers on the right denote the molecular mass of marker proteins in kilodaltons. Experiments were repeated three times with similar results. (C) The interaction of SIUBA1 and SIUBA2 with group IV E2s was detected by yeast two-hybrid. SIUBC8 and the empty prey and bait vectors (EV) were used as control. Interaction was demonstrated by activation of the lacZ reporter gene (blue patches). Photographs were taken 24 h after streaking the yeast cells onto plates containing X-Gal. The low left panel shows ratio of blue color intensity in yeast cell patches of UBA1-E2 compared to that of the UBA2-E2 as shown in upper left panel. The right panel shows comparable level of SlUBA1 and SlUBA2 protein and similar level of the E2 protein were expressed for each pair of SIUBA1-E2 and SIUBA2-E2 in the yeast cells. CBS, Coomassie blue staining as an indicator of equal sample loading. (D) Tomato UBA2 showed significantly stronger interaction with SIUBC32, SIUBC33 and SIUBC34 than UBA1 in the BiFC assay. SIUBC12 was used as control. Images from four random microscopic fields for each tested construct pair were presented. The experiment was repeated two times with similar results. Scale bar = 20 µm. Low panel shows the level of protein expressed in planta for the E1 (UBA1 or UBA2)-E2 pairs tested in the assay. (E) and (F) Significantly higher amount of tomato UBA2 than UBA1 was pulled down by SlUBC32, SlUBC33 and SlUBC34 in coimmunoprecipitation assay, FLAG-tagged SIUBC12 and GFP were used as negative controls. The experiment was repeated two times with similar result.

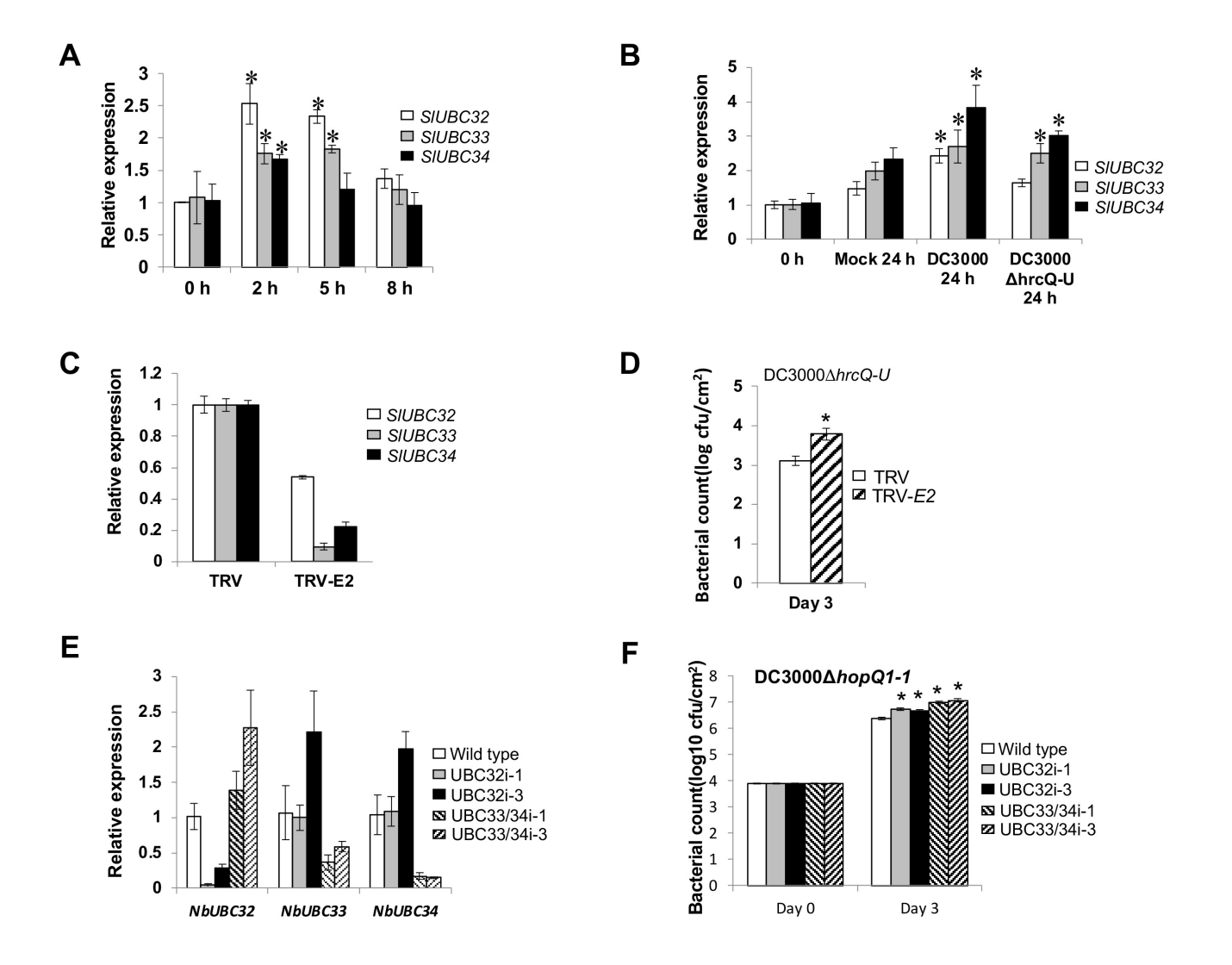


Figure 3. Group IV E2s are required for plant immunity. (A) and (B) The expression of tomato SIUBC32, 33 and 34 genes was induced by flg22 (A) and different Pst strains (B). The expression of SlUBC32, SlUBC33 and SlUBC34 were analyzed by qRT-PCR using tomato  $EF1\alpha$  gene as the internal reference. The experiment was performed with three technical repeats in each of the three biological replicates. Error bars indicate standard deviation. Asterisks indicate significantly elevated expression compared to mock plants at the same time point based on the one-way ANOVA (P < 0.01). (C) and (E) The E2 genes were efficiently and specifically silenced in tomato (C) and tobacco (E) plants. The accumulation of the transcript for E2 genes was quantified by qRT-PCR.  $EF1\alpha$  was used as an internal reference. In tomato (C), plants infected with the empty TRV vector were used as control (TRV). In tobacco (E), wild type plants were used as control. The relative quantity of transcript for corresponding gene in control plants was set as 1. Experiments were repeated at least two times with similar results. (D) Knocking down the expression of tomato group IV E2 genes significantly increased bacterial growth (DC3000\(Delta\) hrcQ-U) compared to the control plants infected with the TRV empty vector (TRV). The dipping method was used for pathogen inoculation. (F) Knocking down the expression of tobacco group IV E2 genes in transgenic plants significantly increased bacterial growth (DC3000∆hopQ1-1) compared to the control plants. In (D) and (F), asterisks indicate significantly increased bacterial growth compared to control plants based on the one-way ANOVA (P < 0.01).

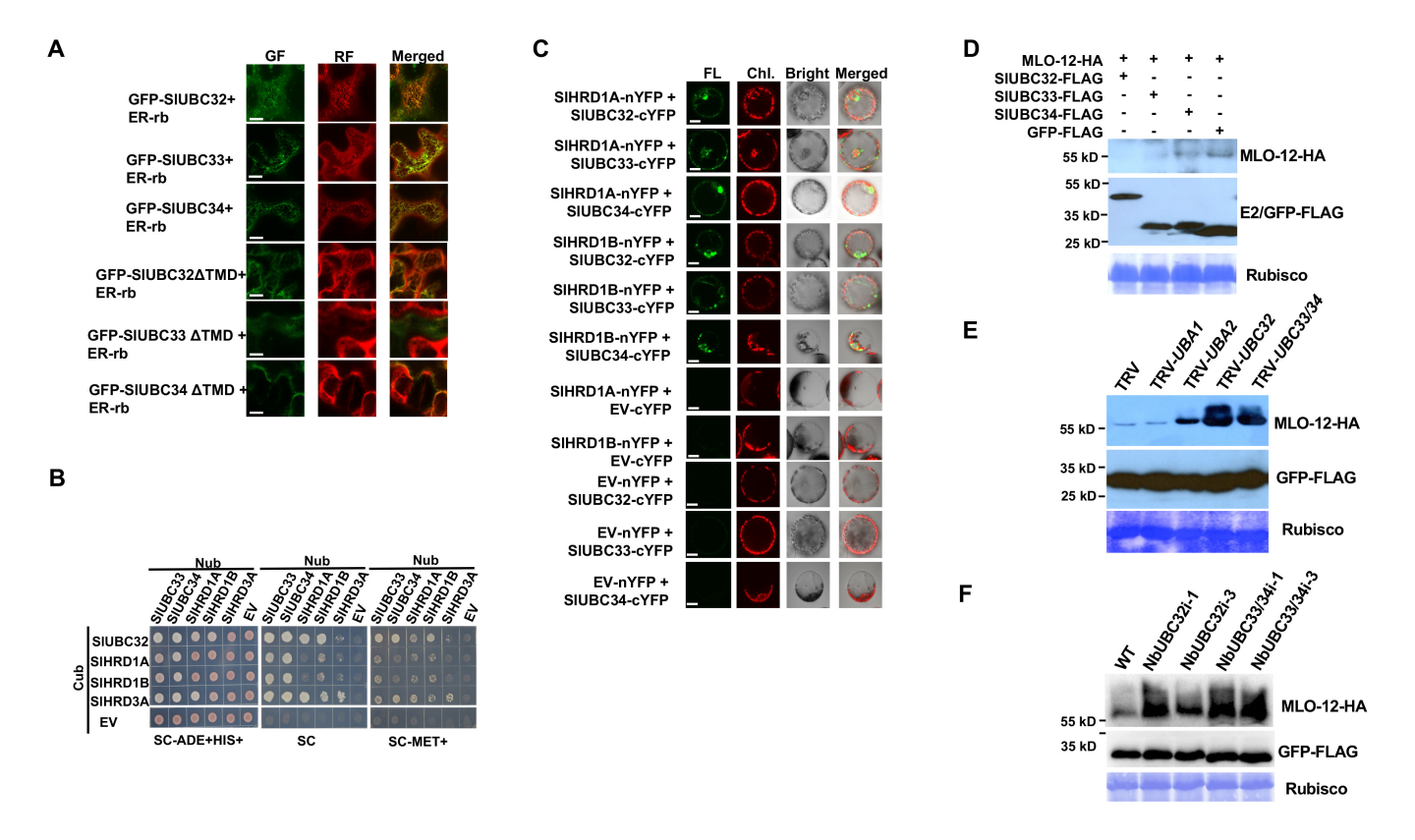


Figure 4. Tomato UBC32, UBC33, and UBC34 are endoplasmic reticulum (ER)-bound and are involved in ERAD. (A) Tomato E2s SlUBC32, SlUBC33 and SlUBC34 are localized to the ER. GFPfused wild type and transmembrane domain-deleted (ΔTMD) mutant version of SIUBC32, SIUBC33 and SIUBC34 were examined using confocal microscope. GF, green fluorescence; RF, red fluorescence conferred by mCherry-ER-localized marker protein (ER-rb). (B) SIUBC32, SIUBC33 and SIUBC34 interacted with tomato homolog of ERAD-associated ubiquitin E3 ligases, SIHRD1A and SIHRD1B and their adapter protein SIHRD3A in the mating-based split ubiquitin yeast two-hybrid system. Growth of yeast cells harboring two genes that had been fused with the N-terminal (Nub) and Cterminal (Cub) halves of the ubiquitin protein, respectively on SC-ADE+HIS+, SC- and SC- with 0.15 M MET media plates, respectively, were shown in the left, middle and right panel. Empty bait and prey vector (EV) were used as control. (C) SIUBC32, SIUBC33 and SIUBC34 interacted with SIHRD1A and SIHRD1B in BiFC assay using tomato leaf protoplasts. EV, empty vector; FL., fluorescence; Chl., chlorophyll autofluorescence; Bright, bright field image. Scale bar = 20 µm. (D) Transient coexpression in N. benthamiana leaves of the group IV E2 and the known ERAD target MLO-12 increased degradation of MLO-12. GFP was used as control. (E) Knocking down UBA2 and group IV E2s in leaves of N. benthamiana plants by VIGS reduced the degradation of MLO-12. (F) Degradation of MLO-12 was reduced in N. benthamiana RNAi transgenic lines where group IV E2 genes was silenced. Two independent transgenic lines in which the NbUBC32 gene and the NbUBC33 and NbUBC34 genes were silenced, respectively were used for the assay. The experiments in (E) and (F) were repeated two times with similar result. In (D), (E) and (F), the FLAG-tagged GFP was expressed together with HA-tagged MLO-12 as an internal control of efficiency in transient expression as well as control of non-misfolded protein. Staining of the Rubisco large subunit (Rubisco) by Coomassie Blue R250 denotes equal sample loading.

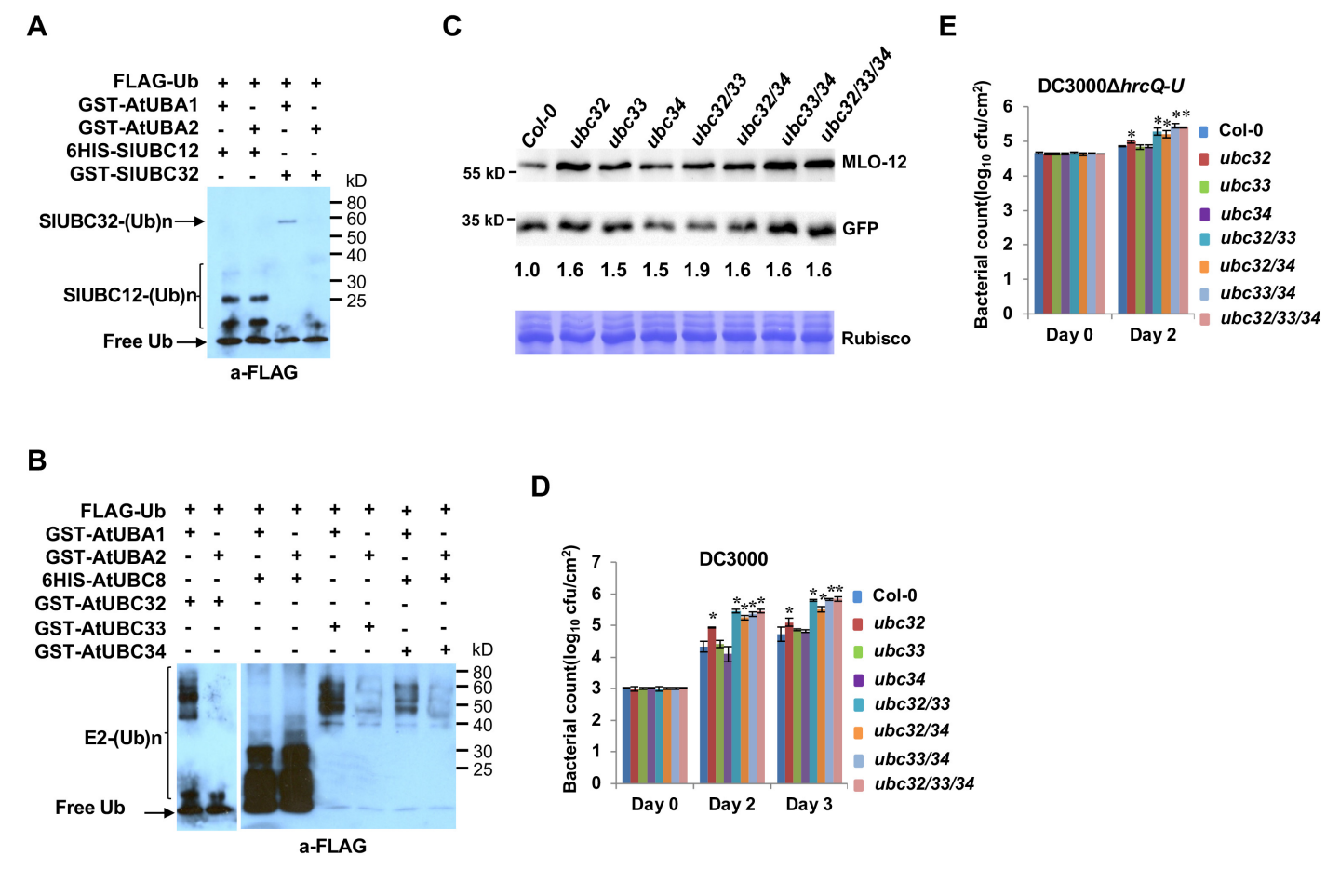


Figure 5. Arabidopsis E2 enzymes AtUBC32, AtUBC33 and AtUBC34 are differentially charged by the E1s AtUBA1 and AtUBA2 and are required for ERAD and host immunity. (A) Tomato SIUBC32 was charged by AtUBA1 with higher specificities than that of AtUBA2 in thioester assay. The tomato SIUBC12 to which tomato E1 display comparable specificities was used as control. (B) The Arabidopsis E2s AtUBC32, AtUBC33 and AtUBC34 were charged by AtUBA1 at significantly higher efficiencies than that of AtUBA2 in thioester assay. The AtUBC8 was used as control. The experiments in (A) and (B) were repeated two times with similar result. (C) Loss of function in AtUBC32, AtUBC33 and AtUBC34 diminished the degradation of MLO-12 by ERAD. MLO-12 was transiently expressed in protoplasts derived from leaves of Col-0 and the mutants, respectively. The GFP-HA was used as internal control for transfection efficiencies. (D) and (E) Bacterial growth assay on single, double and triple mutants of the Arabidopsis mutant ubc32, ubc33 and ubc34. Wild-type Col-0 and different mutants for the AtUBC32, AtUBC33 and AtUBC34 gene were infected with DC3000 (D) and DC3000∆hrcQ-U (E), and then the bacterial population was examined on 2 and 3 days after infection. Bars show standard deviation. Asterisks indicate significantly elevated bacterial growth compared with the WT plants based on one-way ANOVA (P < 0.01). cfu, colony-forming units. The experiments were repeated three times with similar results.

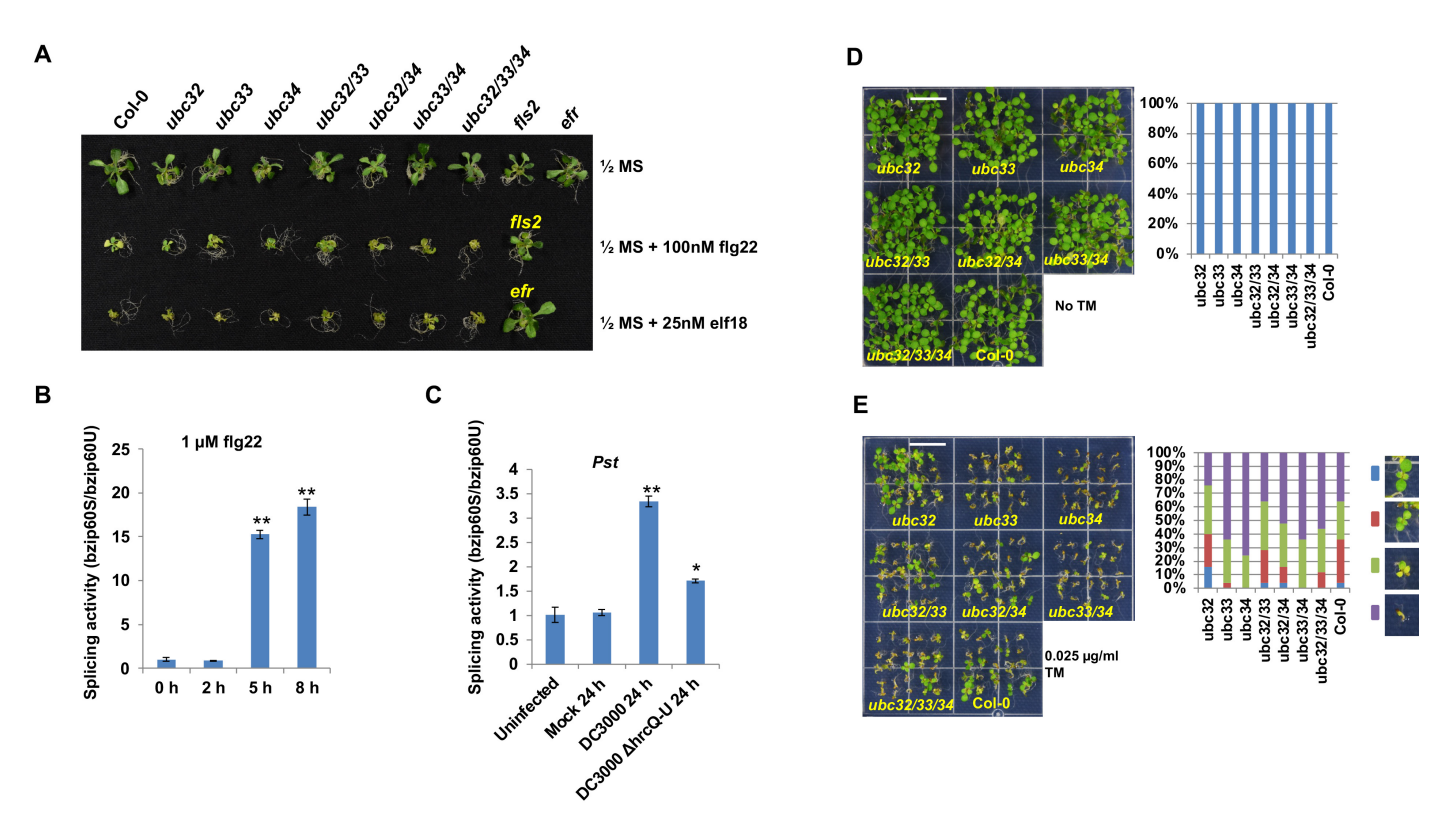


Figure 6. Knocking out AtUBC32, AtUBC33, and At UBC34 do not affect flg22 and elf18triggered seedling growth inhibition but alternate plant ER stress tolerance. (A) Phenotype of wild-type Col-0 and ubc32, ubc33, ubc34 single, double, and triple mutant seedlings untreated or treated with flg22 and elf18. The fls2 and efr mutant were included as control. Similar results were obtained in three independent experiments. (B) and (C) ER stress response is involved in plant immunity. Quantitative measurement of bZIP60 mRNA splicing activity was performed by qRT-PCR analyses of spliced (bzip60S) and non-spliced (bzip60U) bZIP60 forms. Ratios of bzip60S to bzip60U are calculated, with setting the ratio of uninfected Col-0 as 1. (B) qRT-PCR analyses of bzip60S and bzip60U in 10-day tomato seedlings with 1 µM flg22 treatment in ½ liquid MS media were conducted. Ratios of spliced bzip60S and unspliced bzip60U was shown. (C) Ratios of spliced bzip60S and unspliced bzip60U was shown for 3-week tomato plants infected with *Pst* pathogens by dipping method. Statistical analysis was performed using Student's t-test. \*,  $p \le 0.05$ . \*\*,  $p \le 0.001$ . The experiments were performed at least two times with similar results. (D) and (E) The phenotypes of different Arabidopsis ubc32, ubc33 and ubc34 mutant lines grew on media without (**D**) or with 0.025 μg/mL tunicamycin (E) in seedling growth assay. The percentages of different phenotypes are shown in the right panels. A representative image of two independent experiments is shown. For quantification of seedling phenotypes,  $n \ge 30$  (right panel). Bar = 0.5 cm. Photos were taken 7 days after sowing cold stratification-processed seeds on the growth media.

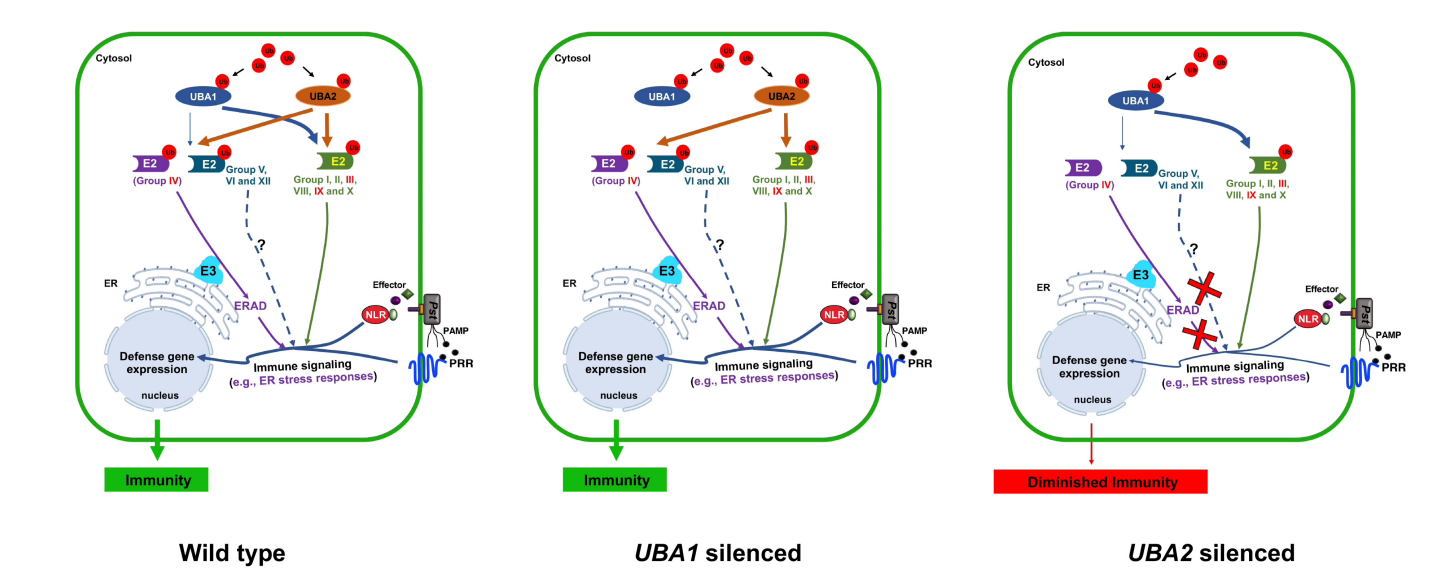


Figure 7. A working model illustrates how the plant DUAS function distinctly in host immunity. The two tomato E1s display comparable specificities to E2s of groups I, II, III, VIII, IX and X. However, UBA2 charges E2s of groups IV, V, VI, and XII with significantly higher specificities, which contribute to the distinct roles of UBA1 and UBA2 in plant growth, development, and defense. In the absence of UBA1, UBA2 can charge the E2s of group I, II, III, VIII, IX and X efficiently and the charging of groups IV, V, VI, and XII E2s is also not affected. By contrast, knocking out UBA2 will significantly reduce the charging of group IV, V, VI, and XII E2s, which in turn will affect cooperation of them with cognate E3s, such as working with ERADrelated E3s by group IV E2s, to modulate cognate plant immunity-related substrates by ubiquitin. Consequently, plant immunity is diminished. Nearly all sequenced plant genomes encode two or more ubiquitin E1s. Thus, plants likely encode dual or multiple E1 activation systems for ubiquitin that do not play equivalent roles in various physiological processes. Fonts in red color denotes that group III, IV, and IX E2s have been shown to modulate plant immunity. The question mark indicates that the role of group V, VI and XII E2s in plant immunity is unclear. Ub, ubiquitin; NLR, nucleotide-binding leucine-rich repeat protein; Pst, Pseudomonas syringae pv. tomato.

#### **Parsed Citations**

Ahn, M.Y., Oh, T.R., Seo, D.H., Kim, J.H., Cho, N.H., and Kim, W.T. (2018). Arabidopsis group XIV ubiquitin-conjugating enzymes AtUBC32, AtUBC33, and AtUBC34 play negative roles in drought stress response. Journal of plant physiology 230, 73-79.

Google Scholar: Author Only Title Only Author and Title

Berner, N., Reutter, K., and Wolf, D. (2018). Protein Quality Control of the Endoplasmic Reticulum and Ubiquitin-Proteasome-Triggered Degradation of Aberrant Proteins: Yeast Pioneers the Path. Annu Rev Biochem 87, 751-782.

Google Scholar: Author Only Title Only Author and Title

Block, K., Boyer, T.G., and Yew, P.R. (2001). Phosphorylation of the human ubiquitin-conjugating enzyme, CDC34, by casein kinase 2. J Biol Chem 276. 41049-41058.

Google Scholar: Author Only Title Only Author and Title

Bombarely, A, Rosli, H.G., Vrebalov, J., Moffett, P., Mueller, L.A, and Martin, G.B. (2012). A draft genome sequence of Nicotiana benthamiana to enhance molecular plant-microbe biology research. Molecular plant-microbe interactions: MOL PLANT MICROBE INTERACT 25, 1523-1530.

Google Scholar: Author Only Title Only Author and Title

Buchberger, A, Bukau, B., and Sommer, T. (2010). Protein quality control in the cytosol and the endoplasmic reticulum: brothers in arms. Molecular cell 40, 238-252.

Google Scholar: Author Only Title Only Author and Title

Callis, J. (2014). The ubiquitination machinery of the ubiquitin system. Arabidopsis Book 12, e0174.

Google Scholar: Author Only Title Only Author and Title

Caplan, J., and Dinesh-Kumar, S.P. (2006). Using viral vectors to silence endogenous genes. In Current protocols in microbiology (John Wiley & Sons, Inc.), pp. 16l.16.11-16l.13.

Google Scholar: Author Only Title Only Author and Title

Chakraborty, R., Uddin, S., Macoy, D.M., Park, S.O., Van Anh, D.T., Ryu, G.R., Kim, Y.H., Lee, J.-Y., Cha, J.-Y., Kim, W.-Y., Lee, S.Y., and Kim, M.G. (2020). Inositol-requiring enzyme 1 (IRE1) plays for AvrRpt2-triggered immunity and RIN4 cleavage in Arabidopsis under endoplasmic reticulum (ER) stress. Plant Physiology and Biochemistry 156, 105-114.

Google Scholar: Author Only Title Only Author and Title

Chakravarthy, S., Velásquez, A.C., Ekengren, S.K., Collmer, A., and Martin, G.B. (2010). Identification of Nicotiana benthamiana Genes Involved in Pathogen-Associated Molecular Pattern-Triggered Immunity. Molecular plant-microbe interactions: MOL PLANT MICROBE INTERACT 23, 715-726.

Google Scholar: Author Only Title Only Author and Title

Chen, B., Mariano, J., Tsai, Y., Chan, A., Cohen, M., and Weissman, A. (2006). The activity of a human endoplasmic reticulum-associated degradation E3, gp78, requires its Cue domain, RING finger, and an E2-binding site. Proc Natl Acad Sci U S A 103, 341-346.

Google Scholar: Author Only Title Only Author and Title

Chen, Q., Yu, F., and Xie, Q. (2020). Insights into endoplasmic reticulum-associated degradation in plants. New Phytol 226, 345-350. Google Scholar: Author Only Title Only Author and Title

Chen, Q., Zhong, Y., Wu, Y., Liu, L., Wang, P., Liu, R., Cui, F., Li, Q., Yang, X., Fang, S., and Xie, Q. (2016). HRD1-mediated ERAD tuning of ER-bound E2 is conserved between plants and mammals. Nature plants 2, 16094.

Google Scholar: <u>Author Only Title Only Author and Title</u>

Cook, J.C., and Chock, P.B. (1995). Phosphorylation of ubiquitin-activating enzyme in cultured cells. Proc Natl Acad Sci U S A 92, 3454-3457.

Google Scholar: Author Only Title Only Author and Title

Cui, F., Liu, L., Li, Q., Yang, C., and Xie, Q. (2012a). UBC32 mediated oxidative tolerance in Arabidopsis. J Genet Genomics 39, 415-417. Google Scholar: Author Only Title Only Author and Title

Cui, F., Liu, L., Zhao, Q., Zhang, Z, Li, Q., Lin, B., Wu, Y., Tang, S., and Xie, Q. (2012b). Arabidopsis ubiquitin conjugase UBC32 is an ERAD component that functions in brassinosteroid-mediated salt stress tolerance. The Plant cell 24, 233-244.

Google Scholar: <u>Author Only Title Only Author and Title</u>

Eaton, B., Gold, L., and Zichi, D. (1995). Let's get specific: the relationship between specificity and affinity. Chem Biol 2, 633-638. Google Scholar: Author Only Title Only Author and Title

Golemis, E.A., Serebriiskii, I., Finley Jr, R.L., Kolonin, M.G., Gyuris, J., and Brent, R. (2008). Interaction trap/two-hybrid system to identify interacting proteins. In Current Protocol in Molecular Biology, F.M. Ausubel, R. Brent, R.E. Kingston, D.D. Moore, J.G. Seidman, J.A Smith, and K. Struhl, eds (New York: John Wiley), pp. 20.21.21-20.21.35.

Google Scholar: Author Only Title Only Author and Title

Gómez-Gómez, L., and Boller, T. (2000). FLS2: an LRR receptor-like kinase involved in the perception of the bacterial elicitor flagellin in Arabidopsis. Molecular cell 5, 1003-1011.

Google Scholar: Author Only Title Only Author and Title

Goritschnig, S., Zhang, Y., and Li, X. (2007). The ubiquitin pathway is required for innate immunity in Arabidopsis. Plant J 49, 540-551.

Google Scholar: Author Only Title Only Author and Title

Grefen, C., Obrdlik, P., and Harter, K. (2009). The determination of protein-protein interactions by the mating-based split-ubiquitin system (mbSUS). Methods in molecular biology 479, 217-233.

Google Scholar: Author Only Title Only Author and Title

Guerriero, C., and Brodsky, J. (2012). The delicate balance between secreted protein folding and endoplasmic reticulum-associated degradation in human physiology. Physiol Rev 92, 537-576.

Google Scholar: Author Only Title Only Author and Title

Hatfield, P.M., and Vierstra, R.D. (1992). Multiple forms of ubiquitin-activating enzyme E1 from wheat. Identification of an essential cysteine by in vitro mutagenesis. J Biol Chem 267, 14799-14803.

Google Scholar: Author Only Title Only Author and Title

Hatfield, P.M., Gosink, M.M., Carpenter, T.B., and Vierstra, R.D. (1997). The ubiquitin-activating enzyme (E1) gene family in Arabidopsis thaliana. Plant J 11, 213-226.

Google Scholar: Author Only Title Only Author and Title

Jahngen-Hodge, J., Obin, M.S., Gong, X., Shang, F., Nowell, T.R., Jr., Gong, J., Abasi, H., Blumberg, J., and Taylor, A (1997). Regulation of ubiquitin-conjugating enzymes by glutathione following oxidative stress. J Biol Chem 272, 28218-28226.

Google Scholar: Author Only Title Only Author and Title

Jin, J., Li, X., Gygi, S.P., and Harper, J.W. (2007). Dual E1 activation systems for ubiquitin differentially regulate E2 enzyme charging. Nature 447, 1135-1138.

Google Scholar: Author Only Title Only Author and Title

Katagiri, F., Thilmony, R., and He, S.Y. (2002). The Arabidopsis thaliana-pseudomonas syringae interaction. The arabidopsis book 1, e0039.

Google Scholar: Author Only Title Only Author and Title

Kong, S.K., and Chock, P.B. (1992). Protein ubiquitination is regulated by phosphorylation. An in vitro study. J Biol Chem 267, 14189-14192.

Google Scholar: Author Only Title Only Author and Title

Kraft, E., Stone, S.L., Ma, L., Su, N., Gao, Y., Lau, O.-S., Deng, X.-W., and Callis, J. (2005). Genome analysis and functional characterization of the E2 and RING-type E3 ligase ubiquitination enzymes of Arabidopsis. Plant Physiol 139, 1597-1611.

Google Scholar: Author Only Title Only Author and Title

Kunze, G., Zipfel, C., Robatzek, S., Niehaus, K., Boller, T., and Felix, G. (2004). The N terminus of bacterial elongation factor Tu elicits innate immunity in Arabidopsis plants. Plant Cell 16, 3496-3507.

Google Scholar: Author Only Title Only Author and Title

Kvitko, B.H., Park, D.H., Velásquez, AC., Wei, C.-F., Russell, AB., Martin, G.B., Schneider, D.J., and Collmer, A (2009). Deletions in the Repertoire of Pseudomonas syringae pv. tomato DC3000 Type III Secretion Effector Genes Reveal Functional Overlap among Effectors. PLoS Pathog 5, e1000388.

Google Scholar: Author Only Title Only Author and Title

Larkin, M.A, Blackshields, G., Brown, N.P., Chenna, R., McGettigan, P.A, McWilliam, H., Valentin, F., Wallace, I.M., Wilm, A, Lopez, R., Thompson, J.D., Gibson, T.J., and Higgins, D.G. (2007). Clustal W and Clustal X version 2.0. Bioinformatics 23, 2947-2948.

Google Scholar: Author Only Title Only Author and Title

Lee, I., and Schindelin, H. (2008). Structural insights into E1-catalyzed ubiquitin activation and transfer to conjugating enzymes. Cell 134, 268-278.

Google Scholar: <u>Author Only Title Only Author and Title</u>

Li, C., Xia, B., Wang, S., and Xu, J. (2020). Folded or Degraded in Endoplasmic Reticulum. In Regulation of Cancer Immune Checkpoints, Jie Xu, ed (Singapore: Springer), pp. 265-294.

Google Scholar: Author Only Title Only Author and Title

Li, J., Zhao-Hui, C., Batoux, M., Nekrasov, V., Roux, M., Chinchilla, D., Zipfel, C., and Jones, J.D. (2009). Specific ER quality control components required for biogenesis of the plant innate immune receptor EFR. Proc Natl Acad Sci U S A 106, 15973-15978.

Google Scholar: Author Only Title Only Author and Title

Lv, Z, Rickman, K.A, Yuan, L., Williams, K., Selvam, S.P., Woosley, A.N., Howe, P.H., Ogretmen, B., Smogorzewska, A, and Olsen, S.K. (2017). S. pombe Uba1-Ubc15 Structure Reveals a Novel Regulatory Mechanism of Ubiquitin E2 Activity. Mol Cell 65, 699-714 e696.

Google Scholar: Author Only Title Only Author and Title

Moreno, A, Mukhtar, M., Blanco, F., Boatwright, J., Moreno, I., Jordan, M., Chen, Y., Brandizzi, F., Dong, X., Orellana, A, and Pajerowska-Mukhtar, K. (2012). IRE1/bZIP60-mediated unfolded protein response plays distinct roles in plant immunity and abiotic stress responses. PLoS One 7, e31944.

Google Scholar: Author Only Title Only Author and Title

Muller, J., Piffanelli, P., Devoto, A, Miklis, M., Elliott, C., Ortmann, B., Schulze-Lefert, P., and Panstruga, R. (2005). Conserved ERAD-like quality control of a plant polytopic membrane protein. The Plant cell 17, 149-163.

Google Scholar: Author Only Title Only Author and Title

Mural, R.V., Liu, Y., Rosebrock, T.R., Brady, J.J., Hamera, S., Connor, R.A, Martin, G.B., and Zeng, L. (2013). The tomato Fni3 lysine-63-specific ubiquitin-conjugating enzyme and suv ubiquitin E2 variant positively regulate plant immunity. The Plant cell 25, 3615-3631.

Google Scholar: Author Only Title Only Author and Title

Nei, M., and Kumar, S. (2000). Molecular evolution and phylogenetics. (Oxford; New York: Oxford University Press).

Google Scholar: Author Only Title Only Author and Title

Nekrasov, V., Li, J., Batoux, M., Roux, M., Chu, Z.H., Lacombe, S., Rougon, A., Bittel, P., Kiss-Papp, M., Chinchilla, D., van Esse, H.P., Jorda, L., Schwessinger, B., Nicaise, V., Thomma, B.P., Molina, A., Jones, J.D., and Zipfel, C. (2009). Control of the pattern-recognition receptor EFR by an ER protein complex in plant immunity. EMBO J 28, 3428-3438.

Google Scholar: Author Only Title Only Author and Title

Nelson, B.K., Cai, X., and Nebenfuhr, A (2007). Amulticolored set of in vivo organelle markers for co-localization studies in Arabidopsis and other plants. Plant J 51, 1126-1136.

Google Scholar: Author Only Title Only Author and Title

Nguyen, H.P., Chakravarthy, S., Velasquez, A.C., McLane, H.L., Zeng, L., Nakayashiki, H., Park, D.H., Collmer, A., and Martin, G.B. (2010). Methods to study PAMP-triggered immunity using tomato and Nicotiana benthamiana. Molecular plant-microbe interactions: MOL PLANT MICROBE INTERACT 23, 991-999.

Google Scholar: Author Only Title Only Author and Title

Olsen, S.K., and Lima, C.D. (2013). Structure of a ubiquitin E1-E2 complex: insights to E1-E2 thioester transfer. Molecular cell 49, 884-896.

Google Scholar: Author Only Title Only Author and Title

Saijo, Y., Tintor, N., Lu, X., Rauf, P., Pajerowska-Mukhtar, K., Haweker, H., Dong, X., Robatzek, S., and Schulze-Lefert, P. (2009). Receptor quality control in the endoplasmic reticulum for plant innate immunity. EMBO J 28, 3439-3449.

Google Scholar: Author Only Title Only Author and Title

Sambrook, J., and Russell, D.W. (2001). Molecular cloning: a laboratory manual. (Cold Spring Harbor, N.Y.: Cold Spring Harbor Laboratory).

Google Scholar: Author Only Title Only Author and Title

Schäfer, A, Kuhn, M., and Schindelin, H. (2014). Structure of the ubiquitin-activating enzyme loaded with two ubiquitin molecules. Acta Crystallogr D Biol Crystallogr 70, 1311-1320.

Google Scholar: Author Only Title Only Author and Title

Schulman, B.A, and Harper, J.W. (2009). Ubiquitin-like protein activation by E1 enzymes: the apex for downstream signalling pathways. Nat. Rev. Mol. Cell Biol. 10, 319-331.

Google Scholar: <u>Author Only</u> <u>Title Only</u> <u>Author and Title</u>

Stephen, A.G., Trausch-Azar, J.S., Ciechanover, A., and Schwartz, A.L. (1996). The ubiquitin-activating enzyme E1 is phosphorylated and localized to the nucleus in a cell cycle-dependent manner. J Biol Chem 271, 15608-15614.

Google Scholar: <u>Author Only Title Only Author and Title</u>

Strasser, R. (2018). Protein Quality Control in the Endoplasmic Reticulum of Plants. Annu Rev Plant Biol 69, 147-172.

Google Scholar: Author Only Title Only Author and Title

Takizawa, M., Goto, A, and Watanabe, Y. (2005). The tobacco ubiquitin-activating enzymes NtE1A and NtE1B are induced by tobacco mosaic virus, wounding and stress hormones. Mol Cells 19, 228-231.

Google Scholar: Author Only Title Only Author and Title

Tamura, K., Stecher, G., Peterson, D., Filipski, A, and Kumar, S. (2013). MEGA6: Molecular Evolutionary Genetics Analysis version 6.0. Mol Biol Evol 30, 2725-2729.

Google Scholar: <u>Author Only Title Only Author and Title</u>

The tomato genome Consortium. (2012). The tomato genome sequence provides insights into fleshy fruit evolution. Nature 485, 635-641.

Google Scholar: Author Only Title Only Author and Title

Vierstra, R.D. (2003). The ubiquitin/26S proteasome pathway, the complex last chapter in the life of many plant proteins. Trends Plant Sci. 8, 135-142.

Google Scholar: Author Only Title Only Author and Title

Wang, D., Weaver, N., Kesarwani, M., and Dong, X. (2005). Induction of protein secretory pathway is required for systemic acquired resistance. Science 308, 1036-1040.

Google Scholar: Author Only Title Only Author and Title

Wei, C.-F., Kvitko, B.H., Shimizu, R., Crabill, E., Alfano, J.R., Lin, N.-C., Martin, G.B., Huang, H.-C., and Collmer, A (2007). A Pseudomonas syringae pv. tomato DC3000 mutant lacking the type III effector HopQ1-1 is able to cause disease in the model plant

Nicotiana benthamiana. Plant J 51, 32-46.

Google Scholar: Author Only Title Only Author and Title

Wierzba, M.P., and Tax, F.E. (2016). An Allelic Series of bak1 Mutations Differentially Alter bir1 Cell Death, Immune Response, Growth, and Root Development Phenotypes in Arabidopsis thaliana. Genetics 202, 689-702.

Google Scholar: Author Only Title Only Author and Title

Yu, X., Feng, B., He, P., and Shan, L. (2017). From Chaos to Harmony: Responses and Signaling upon Microbial Pattern Recognition. Annual Review of Phytopathology 55, 109-137.

Google Scholar: Author Only Title Only Author and Title

Zhang, C., Song, L., Choudhary, M.K., Zhou, B., Sun, G., Broderick, K., Giesler, L., and Zeng, L. (2018). Genome-wide analysis of genes encoding core components of the ubiquitin system in soybean (Glycine max) reveals a potential role for ubiquitination in host immunity against soybean cyst nematode. BMC plant biology 18, 149.

Google Scholar: Author Only Title Only Author and Title

Zhang, Y., and Zeng, L. (2020). Crosstalk between Ubiquitination and Other Post-translational Protein Modifications in Plant Immunity. Plant Communications, 100041.

Google Scholar: Author Only Title Only Author and Title

Zhou, B., and Zeng, L. (2017). Elucidating the role of highly homologous Nicotiana benthamiana ubiquitin E2 gene family members in plant immunity through an improved virus-induced gene silencing approach. Plant Methods 13, 59.

Google Scholar: Author Only Title Only Author and Title

Zhou, B., Mural, R.V., Chen, X., Oates, M.E., Connor, R.A, Martin, G.B., Gough, J., and Zeng, L. (2017). A Subset of Ubiquitin-Conjugating Enzymes is Essential for Plant Immunity. Plant Physiol 173, 1371-1390.

Google Scholar: Author Only Title Only Author and Title

Zipfel, C., Robatzek, S., Navarro, L., Oakeley, E.J., Jones, J.D.G., Felix, G., and Boller, T. (2004). Bacterial disease resistance in Arabidopsis through flagellin perception. Nature 428, 764-767.

Google Scholar: Author Only Title Only Author and Title

Zipfel, C., Kunze, G., Chinchilla, D., Caniard, A., Jones, J.D.G., Boller, T., and Felix, G. (2006). Perception of the bacterial PAMP EF-Tu by the receptor EFR restricts Agrobacterium-mediated transformation. Cell 125, 749-760.

Google Scholar: Author Only Title Only Author and Title